JOURNAL OF GEOPHYSICAL RESEARCH, VOL. 99, NO. B12, PAGES 23,801–23,825, DECEMBER 10, 1994

The Krafla spreading segment, Iceland 1. Three-dimensional crustal structure and the spatial and temporal distribution of local earthquakes

S. K. Arnott
Shell International Petroleum Company, The Hague, Netherlands

G. R. Foulger[1]
Department of Geological Sciences, University of Durham, Durham, England

Abstract. The geothermal seismicity of the Krafla Volcanic System, NE Iceland, was monitored for 3 months in 1985 using a dense, local seismometer network. The seismicity was continuous, and the spatial and temporal distributions were roughly known prior to monitoring. The instruments could thereby be deployed in a well-positioned array. A total of 489 locatable events were recorded within the network, and 1771 arrival times were inverted to calculate the three-dimensional P-wave velocity structure and hypocentral locations. Low-velocity volumes were imaged beneath the Krafla and Námafjall geothermal areas and indicate zones of hydrothermal alteration. High-velocity bodies beneath the Krafla caldera rim are interpreted as gabbroic intrusions. Using a three-dimensional velocity structure instead of a refraction-based one-dimensional model to locate the hypocenters significantly improves their location quality and illustrates the shortcomings of using refraction-based models to locate earthquakes in local, anomalous areas. Seismic activity was concentrated within the Krafla and Námafjall geothermal areas and in a narrow zone where dike injections had occurred 8 and 5 years earlier. The activity occurred in the depth range 0-3 km. The seismic rate for the whole area was one magnitude 3.2 event per year and the b value was 0.77 ± 0.10. Most of the seismicity appears to result from geothermal processes in the manner proposed for other Icelandic areas (Foulger and Long, 1984; Foulger, 1988b). Seismicity directly beneath the Bjarnarflag well field within the Námafjall area is probably induced partly by geothermal exploitation. Considerable seismicity also occurred immediately below Leirhnjúkur, a site of intense geothermal activity in the center of the Krafla caldera that overlies a roof pendant in the magma chamber below. This volume of high seismicity is probably highly fractured and may provide a conduit for magma escaping from the magma chamber.

Introduction

Study of the seismicity of accretionary plate boundaries is hampered by the fact that most of them are beneath the ocean. Large earthquakes detectable at teleseismic distances may be studied [e.g., *Sykes*, 1967; *Francis*, 1968], and ocean bottom seismometers (OBSs) yield information about microseismicity [e.g., *Toomey et al.*, 1988]. However, at teleseismic distances only events of magnitude 5 or so are detectable, and OBSs can be deployed for no more than a few weeks and usually in small numbers. These limitations in our monitoring capabilities result in virtually nothing being known about the medium-magnitude seismicity of accretionary plate boundaries, which requires the deployment of regional networks for a few years. In addition, very little is known about the small-magnitude seismicity, which requires dense, well-positioned seismometer arrays. These difficulties are serious barriers to our understanding of the magmatic and hydrothermal processes, three-dimensional crustal structure, crustal stress, and mechanism of rifting at accretionary plate boundaries.

Although the subaerial accretionary plate boundary of Iceland is anomalous, it nevertheless provides a unique opportunity to study ridge seismicity at close hand and free from the inconveniences of marine-based work. The Icelandic landmass is about 300×500 km in size and over 700 km of plate boundary are exposed, including

[1]Currently on leave at Branch of Seismology, U.S. Geological Survey, Menlo Park, California.

Paper number 94JB01465.
0148-0227/94/94JB-01465$05.00

more than 20 spreading segments [*Sæmundsson*, 1979]. A permanent seismometer network has been recording for about 20 years, and the detection threshold for the whole country is about magnitude 2 (P. Einarsson, personal communication, 1985). Data recorded during a recent spreading episode in the Krafla segment [e.g., *Björnsson et al.*, 1977; *Einarsson*, 1978; *Brandsdóttir and Einarsson*, 1979; *Einarsson and Brandsdóttir*, 1980] and accompanying the frequent volcanic eruptions that occur within the neovolcanic zone [e.g., *Gudmundsson et al.*, 1992] have brought sharply into focus the radical improvement in our understanding of crustal accretion that detailed seismological information brings.

In addition to regional networks, dense, local networks have been deployed temporarily in areas of interest for short periods [e.g., *Klein et al.*, 1977]. Icelandic spreading segments generally contain a central volcano and associated high-temperature geothermal area [*Sæmundsson*, 1979]. Many of these generate continuous, small-magnitude earthquake activity with a fixed spatial pattern that is associated with hydrothermal processes [*Foulger and Long*, 1984]. This offers the opportunity to conduct well-conditioned studies of the seismicity, mode of fracture, stress state and crustal structure of those systems because seismometer arrays can be positioned with foreknowledge of the distribution of the earthquakes. Such a study was conducted in 1981 at the Hengill triple junction and geothermal area, SW Iceland, and yielded unique information about the hydrothermal area [*Foulger*, 1988a,b; *Toomey and Foulger*, 1989; *Foulger and Toomey*, 1989].

A dense, 28-station seismometer network was deployed in the Krafla volcanic system for a 3-month period in 1985, immediately following a spreading episode that lasted 1975-1984 [*Björnsson*, 1985]. The experimental objectives were to study the crustal structure of the system and to test the hypothesis that nonshear earthquakes occur there. The location of the continuous seismicity was known, and the instruments were placed around those areas in a regular array. A total of 489 locatable earthquakes were recorded and a simultaneous inversion was conducted to calculate the three-dimensional crustal structure and refined earthquake locations. From these, 153 focal mechanisms were obtained, and these are described by *Arnott and Foulger* [this issue].

The simultaneous inversion indicates that a refraction-derived one-dimensional crustal model that had been in use prior to this study contains systematically low velocities which result in calculated local earthquake hypocenters being up to 700 m too deep. A number of anomalous bodies were detected that correlate well with the surface geology, in particular high-velocity bodies thought to represent intrusions beneath the Krafla caldera rim. The earthquakes were concentrated in the two geothermal areas and in a narrow zone along the center of the fissure swarm where dike injections occurred 8 and 5 years earlier. This correlation of earthquake activity and geothermal activity is typical of Icelandic spreading segments and suggests that the continuous, background seismic activity in the Krafla segment results from geothermal processes as is thought to occur elsewhere in Iceland [*Foulger and Long*, 1984; *Ward and Björnsson*, 1971]. This conclusion is supported by the observation that some of the events had nonshear focal mechanisms with large volumetric components, which indicate the involvement of fluids and/or cavities in the source processes [*Foulger et al.*, 1989; *Arnott*, 1990; *Arnott and Foulger*, this issue].

Tectonics

Iceland Subaerial Regime

The accretionary plate boundary traverses Iceland as a series of en echelon spreading segments, known as "volcanic systems" [*Sæmundsson*, 1979]. Each contains a fissure swarm 10-100 km long and up to 20 km wide consisting of fissures, normal faults, and dikes. Most volcanic systems also contain a central volcano, high-temperature geothermal areas, acid and/or intermediate rocks, and sometimes calderas and magma chambers.

Apart from occasional earthquake sequences, Icelandic spreading segments are mostly quiescent in the short-term except in the high-temperature geothermal areas, where continuous, small-magnitude seismicity often occurs. This contrasts with marine spreading segment seismicity, where frequent small earthquakes are generally recorded irrespective of location along the segment. The seismicity of marine segments thus resembles that of the geothermal areas within Icelandic segments [*Toomey et al.*, 1988; *Ward et al.*, 1969; *Ward and Björnsson*, 1971; *Foulger*, 1982, 1988a].

A detailed seismic study of the Hengill-Grensdalur geothermal area, SW Iceland (Figure 1, inset), revealed a close spatial correlation between the seismicity and the geothermal activity and nonshear focal mechanisms with a large explosive component for many events. They were interpreted as tensile cracking from thermal contraction in the cooling geothermal heat source and therefore induced by the natural geothermal heat loss process [*Foulger and Long*, 1984; *Foulger*, 1988a]. A simultaneous inversion of the data set for three-dimensional structure and hypocentral parameters resolved several high-velocity bodies that were interpreted as gabbroic intrusions and a small, low-velocity body that may contain partial melt [*Toomey and Foulger*, 1989; *Foulger and Toomey*, 1989].

Krafla Volcanic System

Structure and morphology. The Krafla system is one of five en echelon volcanic systems in northeast Iceland (Figure 1). It features a NNE oriented fissure swarm about 10 km wide and 100 km long and a central volcano with a caldera 10 × 8 km, formed during the last interglacial, which ended at 115 ka (Figure 2) [*Sæmundsson*, 1982]. Widespread exposures of rhyolite around the caldera suggest the presence of an underlying magma chamber.

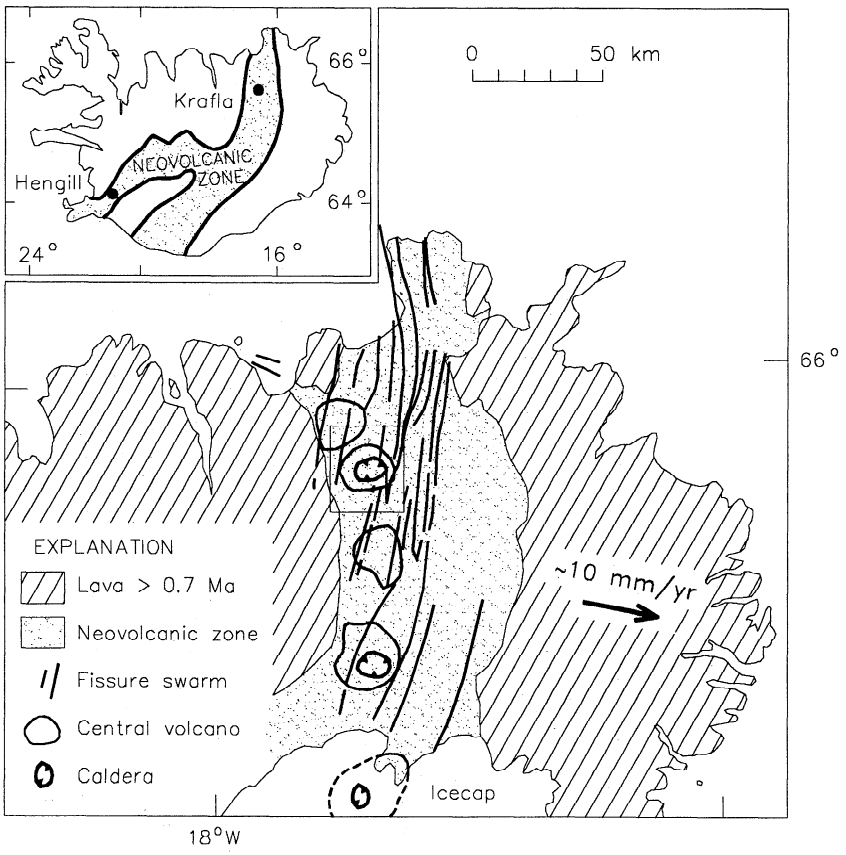

Figure 1. Simplified tectonic map of NW Iceland, showing the elongated en echelon volcanic systems that characterize the neovolcanic zone. Arrow indicates the spreading direction; inset shows the location of the Krafla area within Iceland (adapted from *Björnsson* [1985]). Box indicates area shown in Figure 2.

Two high-temperature geothermal areas exist within this system, the Krafla geothermal area within the caldera and the Námafjall geothermal area 9 km farther south (Figure 2). Both are exploited, the Krafla resource for electric power generation and the Námafjall resource for drying diatomaceous earth. Over 30 geothermal wells have been drilled, and many geophysical and geological studies have been conducted, rendering this a well-studied spreading segment [e.g., *Ragnars et al.*, 1970; *Stefánsson*, 1981; *Ármannsson et al.*, 1987].

The caldera fault has a throw of about 1 km and has been reactivated many times [*Ármannsson et al.*, 1987] and the caldera is filled with hyaloclastites and subaerial lavas. Below about 1300 m, basalt, dolerite, and gabbroic intrusives are dominant, and below 1800 m a gabbro formation underlies the SE caldera rim. The Krafla geothermal area is about 7 km^2 in size and contains a remarkable, intensely geothermally altered ridge Leirhnjúkur containing many hot springs and boiling mud pools (Figure 2). The aquifer-fed reservoir is divided at a depth of $\approx$1 km into an upper, water-dominated zone at 205°C and a lower, boiling zone at 300–350°C.

A magma chamber in the depth interval 3–7 km beneath the caldera is detected by S wave shadows from local earthquakes [*Einarsson*, 1978]. This study suggests that the chamber is divided into two lobes in its upper part (Figure 2), i.e., that the chamber has a roof pendant. Bouguer gravity highs of a few milliGals beneath parts of the caldera rim relative to the center suggest that relatively dense intrusives exist there (Figure 3) [*Karlsdóttir et al.*, 1978], which is supported by borehole data [*Ármannsson et al.*, 1987].

The Námafjall geothermal area is about 4 km^2 in size (Figure 2), and it too contains an intensely geothermally altered ridge, Námafjall, on the western side of which is the main well field, Bjarnarflag. The shallow structure comprises hyaloclastites and basalts and hydrothermally altered rock below about 500 m [*Ragnars et al.*, 1970]. Continuous, shallow seismicity occurs at both the Krafla and Námafjall geothermal areas [*Ward et al.*, 1969; *Ward and Björnsson*, 1971; P. Einarsson, personal communication, 1985].

Recent tectonic activity. A major rifting episode commenced in the Krafla system in 1975 and continued for about 10 years. The magma chamber be-

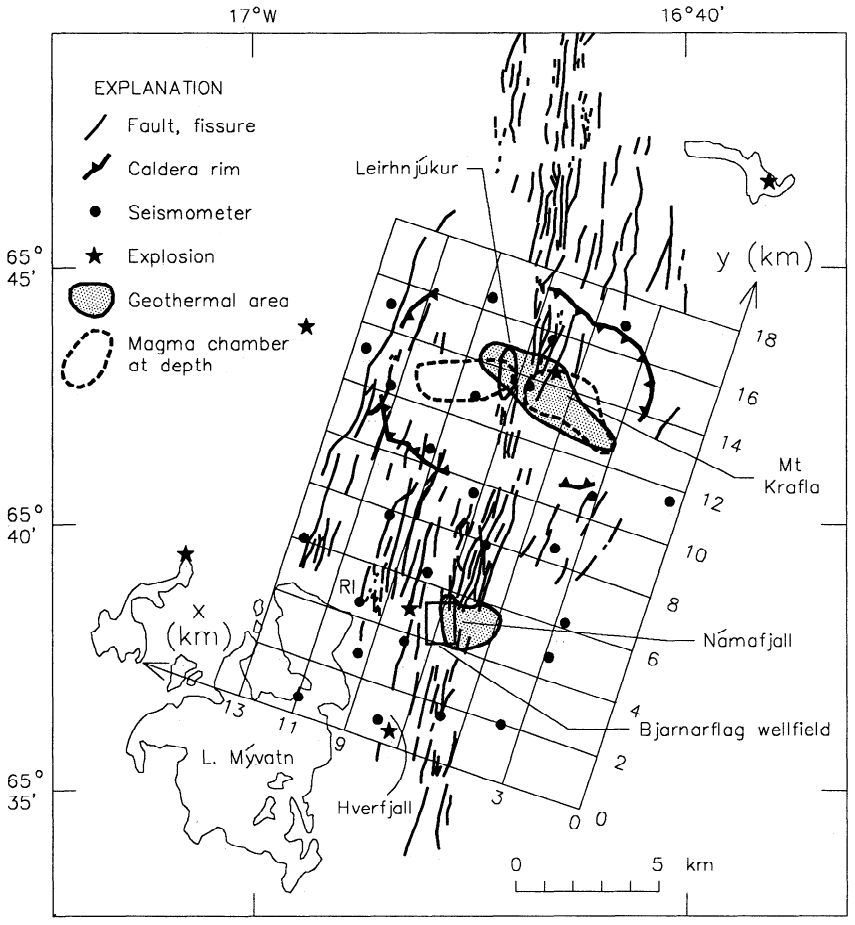

Figure 2. Map of the Krafla area showing tectonic features, the seismometer network deployed in 1985, the locations of the timed explosions, the velocity grid used for the simultaneous inversion, and the place names used in the text. The vertical node spacing was 1 km. Dashed lines indicate magma chamber lobes delineated by S wave shadows [*Einarsson*, 1978]. Box indicates the Bjarnarflag well field. The Krafla geothermal area in the north and the Námafjall geothermal area in the south are shaded.

came activated and repeatedly injected magma laterally into the crust along the fissure swarm forming dikes and lava flows. Each dike injection widened the central part of the fissure swarm by a few tens of centimeters, eventually totaling up to 8 m of extension. Contraction of the flanks occurred in response [e.g., *Björnsson et al.*, 1977, 1979; *Björnsson*, 1985]. Various kinds of seismic activity accompanied this episode, including minor seismic failure in the magma chamber roof during inflation [*Björnsson et al.*, 1977], migrating earthquake swarms that accompanied dike propagation [*Brandsdóttir and Einarsson*, 1978; *Einarsson and Brandsdóttir*, 1980] and volcanic tremor and low-frequency events that were probably associated with surface breakage (P. Einarsson, personal communication, 1982). During quiescent periods, continuous, small earthquakes in the geothermal areas continued to occur, presumably the omnipresent geothermal seismicity.

The recent geological history of the Krafla system is consistent with repetitive tectonism of the kind that occurred 1975–1984. Activity during the last glacial period (115,000-10,000 ka) produced silicic domes and intrusives within and around the caldera. Postglacial volcanism, however, has been mostly basaltic, confined to the caldera and fissure swarm, and occurring at average intervals of 300–500 years [*Thorarinsson*, 1960; *Björnsson et al.*, 1977; *Ármannsson et al.*, 1987]. A single historical volcanic episode, the "Myvatn Fires", of 1724–1729 is thought to have accompanied a spreading episode similar to that which occurred 1975–1984 [*Björnsson et al.*, 1977].

Data Set

Introduction

Seismic monitoring of the Krafla system was conducted in the summer of 1985, after the cessation of the previous decade of tectonic activity. Continuous, small-magnitude seismicity still persisted in the Krafla

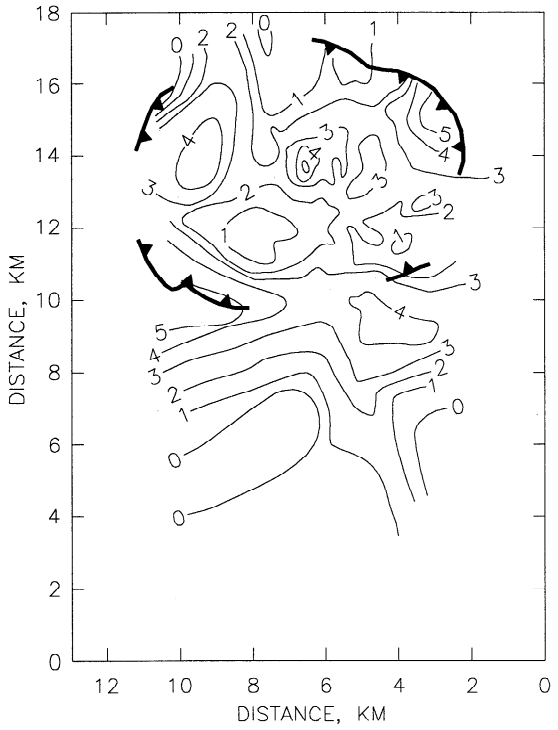

Figure 3. Residual Bouguer gravity map of the Krafla area, calculated using a Bouguer density of 2300 kg m^{-3} and subtracting a north-south linear regional gradient of 0.5 mGal km^{-1}. Contours in milliGals [after *Karlsdóttir et al.*, 1978].

and Námafjall geothermal areas. The approximate distribution of the activity was known, and the equipment was deployed in a good configuration for a focal mechanism study. Data from the nearby permanent drum stations suggested that several hundred locatable events might be expected during a 3-month monitoring period, and this was subsequently found to be the case.

Fieldwork and Data Playback

A network of 27 Willmore Mk. III vertical seismometers with natural periods of 1 s was deployed in an 18 × 13 km area that encompassed the Krafla caldera and the Krafla and Námafjall geothermal areas (Figure 2). The network was operated for 95 days, and data were telemetered using frequency-modulated radio links to GEOSTORE™ recording stations where they were recorded continuously on analog tape along with the MSF radio time signal (broadcast from Rugby, UK) and a clock at each recorder. All the seismometers were installed on bedrock in shallow pits. At the time of the experiment the seismic rate in the Námafjall area was greater than in the Krafla area, and the network was thus made more dense in the south. Six timed explosions were detonated in the area while the equipment was operating, a practice indispensable for reliable determination of the polarity of field instruments, which is critical for focal mechanism studies (Figure 2).

During playback, events were detected aurally, and arrival times were measured by hand from paper records by direct comparison with the radio time pips. More than 500 small local events were processed. The dominant frequency of the signals was about 10 Hz. Arrival times were picked to 0.01 s, and it is estimated that the maximum error in any of the picks, including instrumentally introduced unknowns (e.g., tape recorder head alignments, jet-pen alignments), is about 0.03 s. An example of a well-recorded event is shown by *Arnott and Foulger* [this issue, Figure 2].

Simultaneous Inversion for Three-Dimensional Structure and Hypocentral Parameters

Method

The data comprise a large set of earthquakes recorded on a dense network of seismometers deployed within a relatively small area. They are therefore well suited to simultaneous inversion for both crustal velocity structure and hypocentral parameters. The method of *Thurber* [1983] was used since this treats the velocity structure as a continuous function of space and is more capable of imaging structures with velocity gradients, as are expected in a volcanic area like Krafla, than simpler representations such as an assemblage of blocks of constant velocity.

Thurber's method is described in detail by *Thurber* [1981, 1983, 1984, 1986, 1993]. The study volume is parametrized in terms of seismic speeds at the nodes of a three-dimensional grid (which define the corners of blocks), and linear velocity gradients are assumed between nodes. Starting with a priori values, the program performs a damped, iterative, least squares inversion for hypocentral parameters and the three-dimensional velocity structure.

The problem of coupling of the structure and hypocentral parameters is dealt with by parameter separation which enables the two components to be treated independently, thus greatly reducing the computational burden. The method has been tested extensively using simulated data [e.g., *Kissling*, 1988; *Thurber*, 1981] and found to significantly improve recovery of the true velocity model and hypocentral parameters over methods that hold the hypocenters fixed. The best results are obtained where many ray paths pass through each block along different trajectories, which requires stations distributed throughout the study area and a good distribution of events. Initial starting locations within 2–3 km of the true event positions are desirable [*Thurber*, 1993]. Damping is used to suppress large perturbations in the calculated parameters by a single iteration so that the assumption of piece wise linearity remains acceptable. Thurber's method has been used widely to study small, seismically active volumes of Earth's crust, including a number of volcanic areas, e.g., Kilauea, Hawaii; The Geysers, California; and Hengill, SW Iceland [*Thurber*, 1984; *Eberhart-Phillips*, 1986; *Toomey and Foulger*, 1989].

A subset of earthquakes was selected for the inversion on the basis of data quality as indicated by preliminary location of the events using the program HYPOINVERSE [*Klein*, 1978] with a one-dimensional crustal model obtained by modeling nearby refraction shots (P. Einarsson, personal communication, 1985). Six timed explosions were used along with 105 earthquakes, most of which were recorded on 10 or more seismometers and all of which lay within the network. These provided 1771 P wave arrival times. The locations and origin times of the explosions were held fixed throughout the inversions. The area used for the inversion was selected to compactly enclose the seismometer network and it and the node grid used are shown in Figure 2.

The hypocentral parameters calculated by HYPOINVERSE, and the original one-dimensional model (P. Einarsson, personal communicaton, 1985), were used as initial estimates. A suite of different inversions were performed to study the effect of different input information on the results. The starting velocity model, nodal spacing, and inversion damping value were varied.

The final velocity models calculated invariably contained significantly higher velocities than the original starting model at all depths. A refined one-dimensional crustal model was therefore derived from the results of several trial inversions (Figure 4). This was used as a starting model for the final inversion, although the results were found to be rather insensitive to the a priori model used.

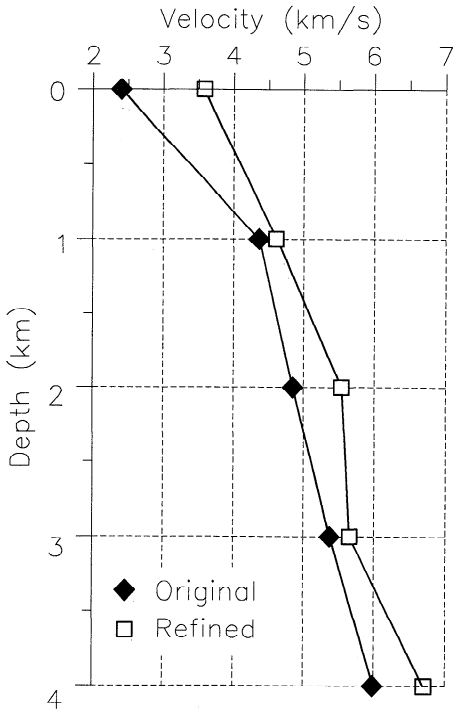

Figure 4. The original one-dimensional velocity model used for location of the hypocenters, and the refined one-dimensional model obtained from the simultaneous inversion.

The nodal spacing used affects the final results, and as it is varied, a trade-off occurs between parameter resolution and data variance reduction. A coarse grid limits the spatial scale of bodies that may be imaged and enables good parameter resolution at the expense of data variance reduction. A fine grid, on the other hand, allows smaller bodies to be imaged, but parameter resolution is lowered, since fewer data constrain each parameter, while data variance reduction is improved. We performed inversions with grid spacings in the horizontal/vertical directions of 2/1 km, 3/2 km, and 4/2 km. For these inversions, the traces of the resolution matrix were 70, 45, and 32; the variance reductions were 84%, 72%, and 61%; and the RMS residuals decreased from an initial 0.066 s to 0.027 s, 0.036 s, and 0.043 s.

The structures obtained using different grid spacings were broadly similar (Figure 5), though some variations in the locations, shapes, and sizes of the anomalies are evident. The coarser parametrizations yield structures on a broader scale than the finer parametrization, a result of velocity averaging. This is clearest in the south of the area, where the two coarse-grid models (Figures 5b and 5c) show broad areas of high and low velocities, whereas the most finely gridded model (Figure 5a) features alternating zones of high and low velocity. In this part of the area the scale of features resolved is similar to the nodal spacing. In the north of the area the most finely gridded model resolves larger-scale bodies and resembles more the coarser models. The grid spacing selected for the final inversion on the basis of these trials was 2/1 km in the horizontal/vertical directions since this corresponded approximately to the surface station spacing, gave a variance reduction down to approximately the estimated maximum data error, and yielded a final model broadly consistent with those from the coarser grids.

Inversions were performed with a suite of damping values. The results were insensitive to values in the range 0.1–2, with RMS errors after seven iterations in the range 0.032 0.036 s. A value of 0.2, which gave the largest variance reduction, was selected for the final inversion. This inversion involved 420 hypocentral and 350 velocity model parameters, iterated seven times and reduced the RMS residual from 0.066 s to 0.027 s. The inversion terminated when additional improvement in the variance reduction with each iteration became less than 7%. The final velocity structure and associated measures of quality are shown in Figures 6 and 7 and Plate 1.

The question of the quality of the final model may be addressed by investigating model uncertainty, resolution, uniqueness, and accuracy. The formal uncertainty of the model (the standard error) is expressed by the roots of the parameter variances, a measure that is usually over-optimistic. *Thurber* [1981] showed that in the case of the method used here, the standard errors may underestimate the true errors by a factor of ≈ 2. The formal uncertainties are mapped alongside the final results in Figure 6. These errors are mostly less than 0.15 km s^{-1}, indicating a true error of up to about

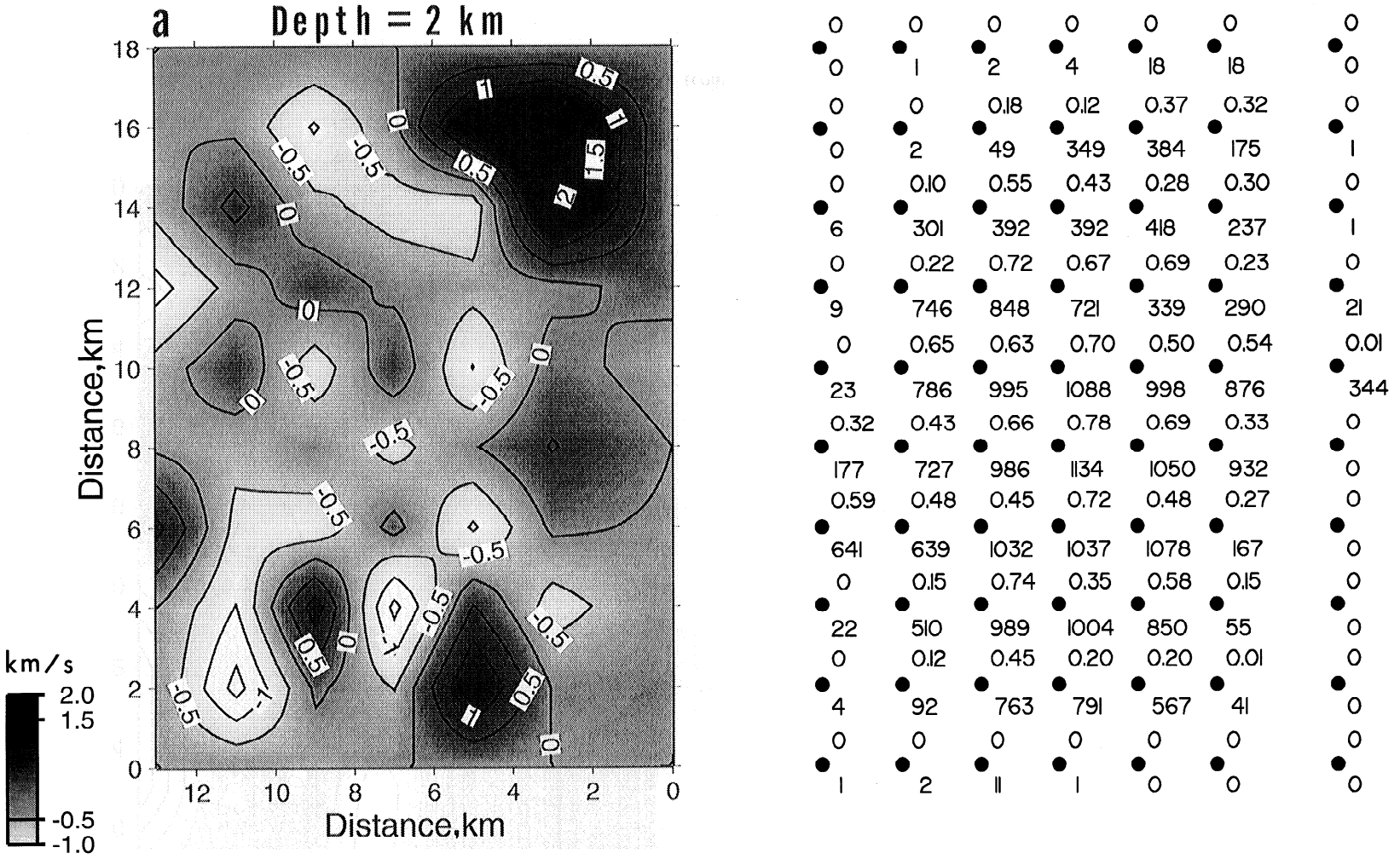

Figure 5. Contoured, grey-shaded plots of a plane at 2 km depth showing the change in velocity (in kilometers per second) from the refined one-dimensional model as a result of the simultaneous inversion. Dark areas indicate high velocities and light areas indicate low velocities. On the right, grids of dots are shown, representing the nodal array used. The diagonal element of the resolution matrix is shown above each dot and the number of rays passing close to the node is shown below each dot. Horizontal/vertical nodal spacings used were (a) 2/1 km, (b) 3/2 km, and (c) 4/2 km.

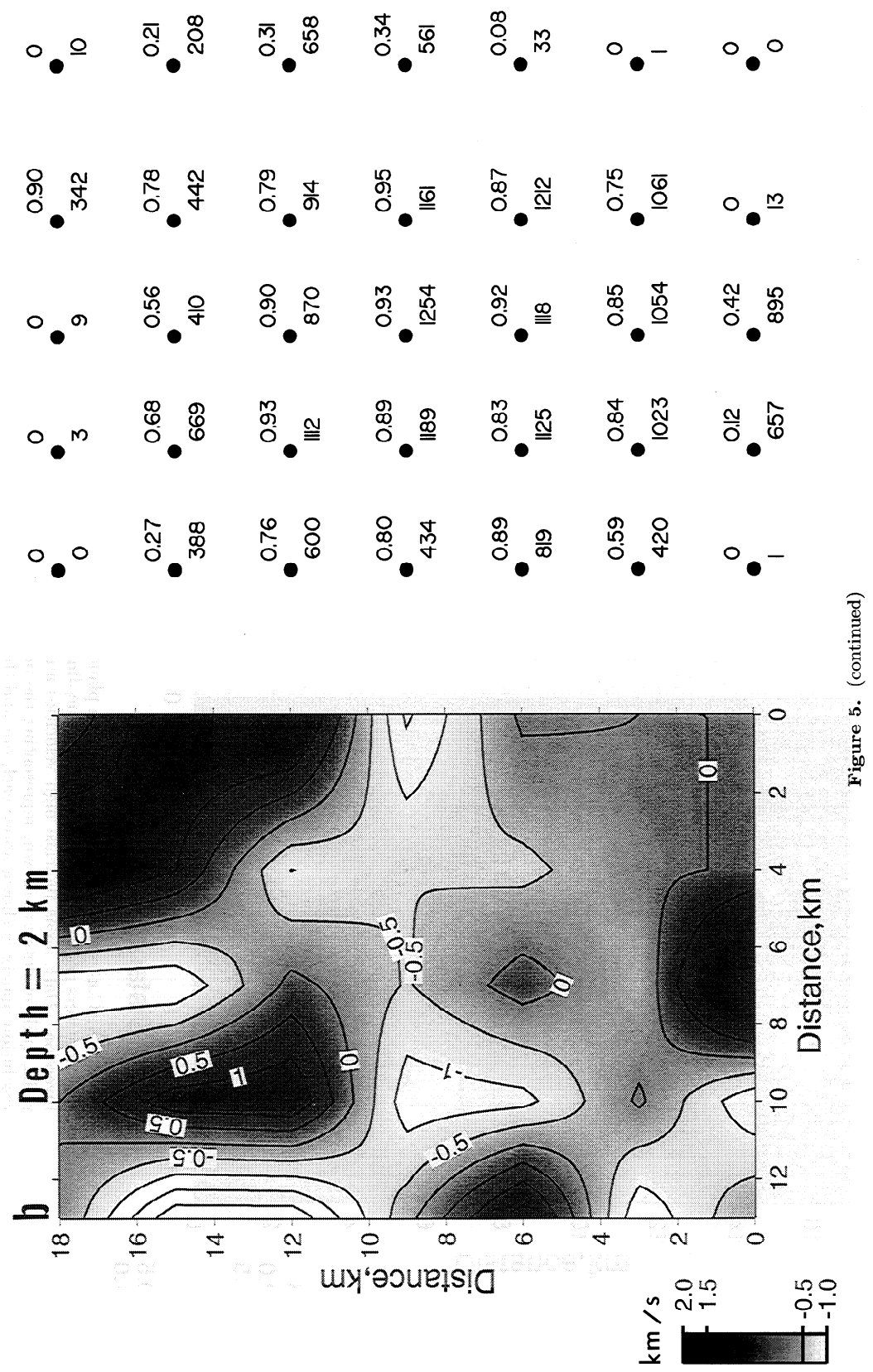

Figure 5. (continued)

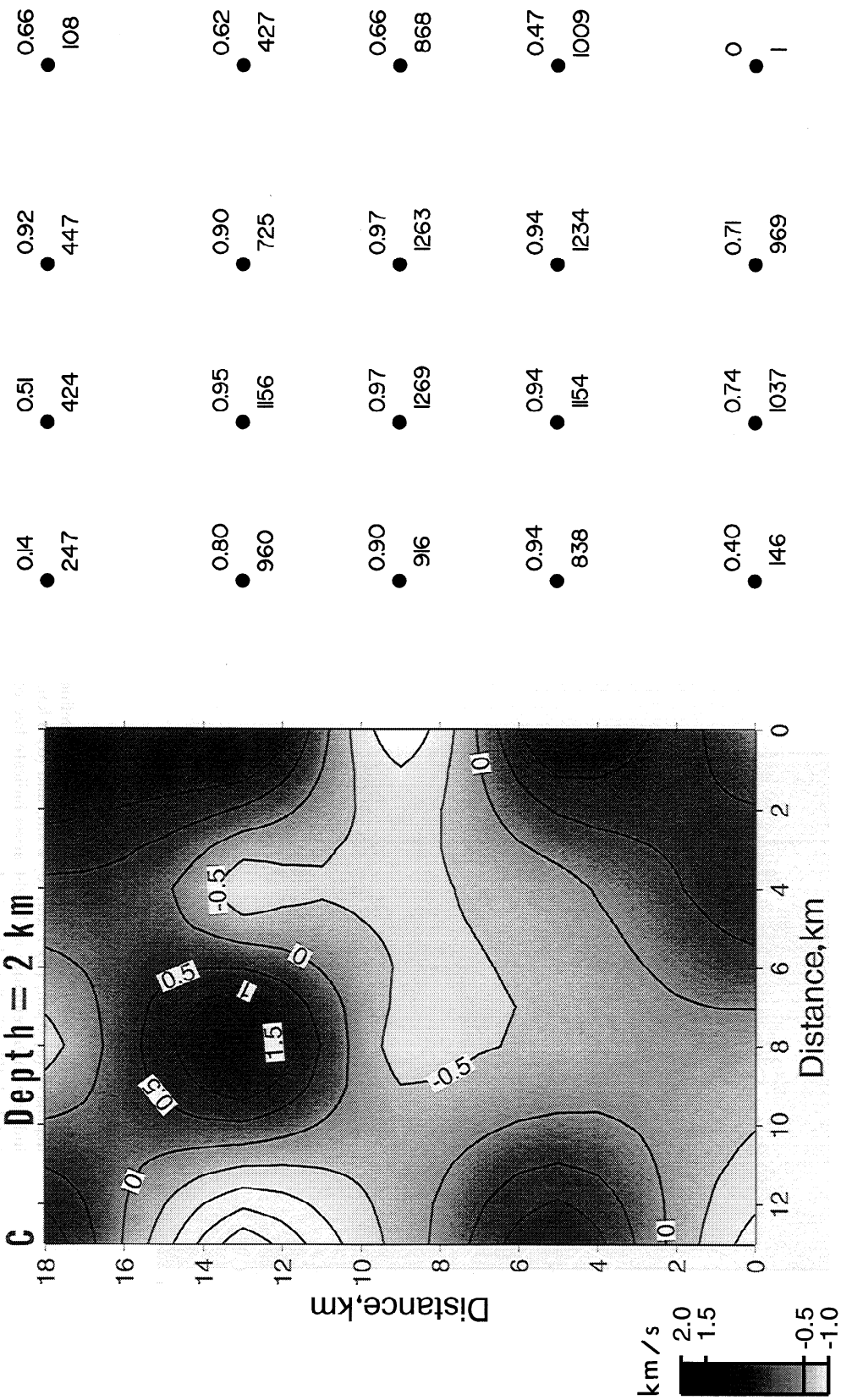

Figure 5. (continued)

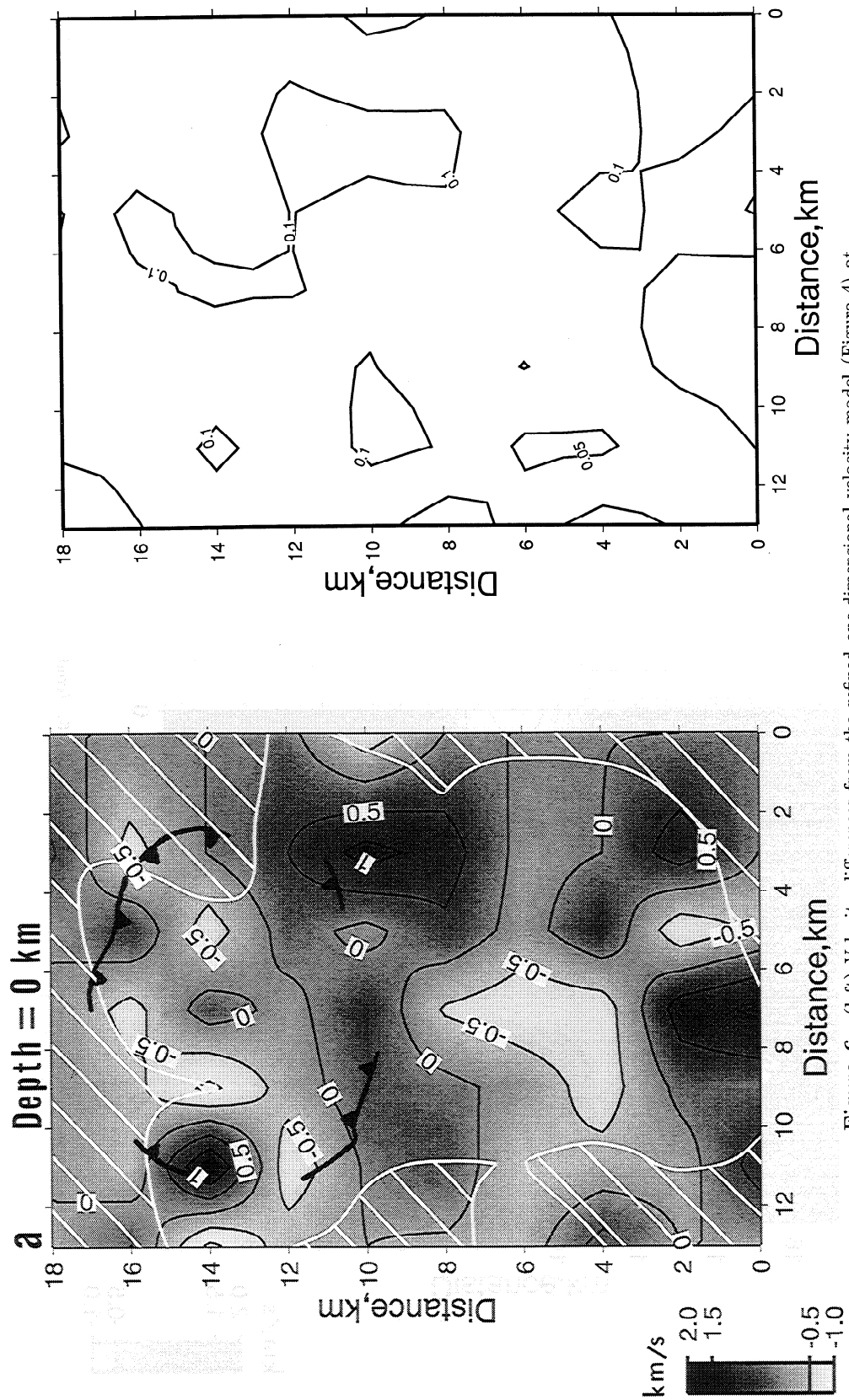

Figure 6. (left) Velocity differences from the refined one-dimensional velocity model (Figure 4) at depths of (a) 0 km, (b) 1 km, (c) 2 km, and (d) 3 km. The contour interval is 0.5 km s^{-1}. Dark areas indicate high velocities and light areas indicate low velocities. Poorly resolved areas (DWS < 50) are hatched. The Krafla caldera is shown.
(right) Contoured maps of model uncertainty (parameter standard errors) for each depth. Contour interval is 0.05 km s^{-1}.

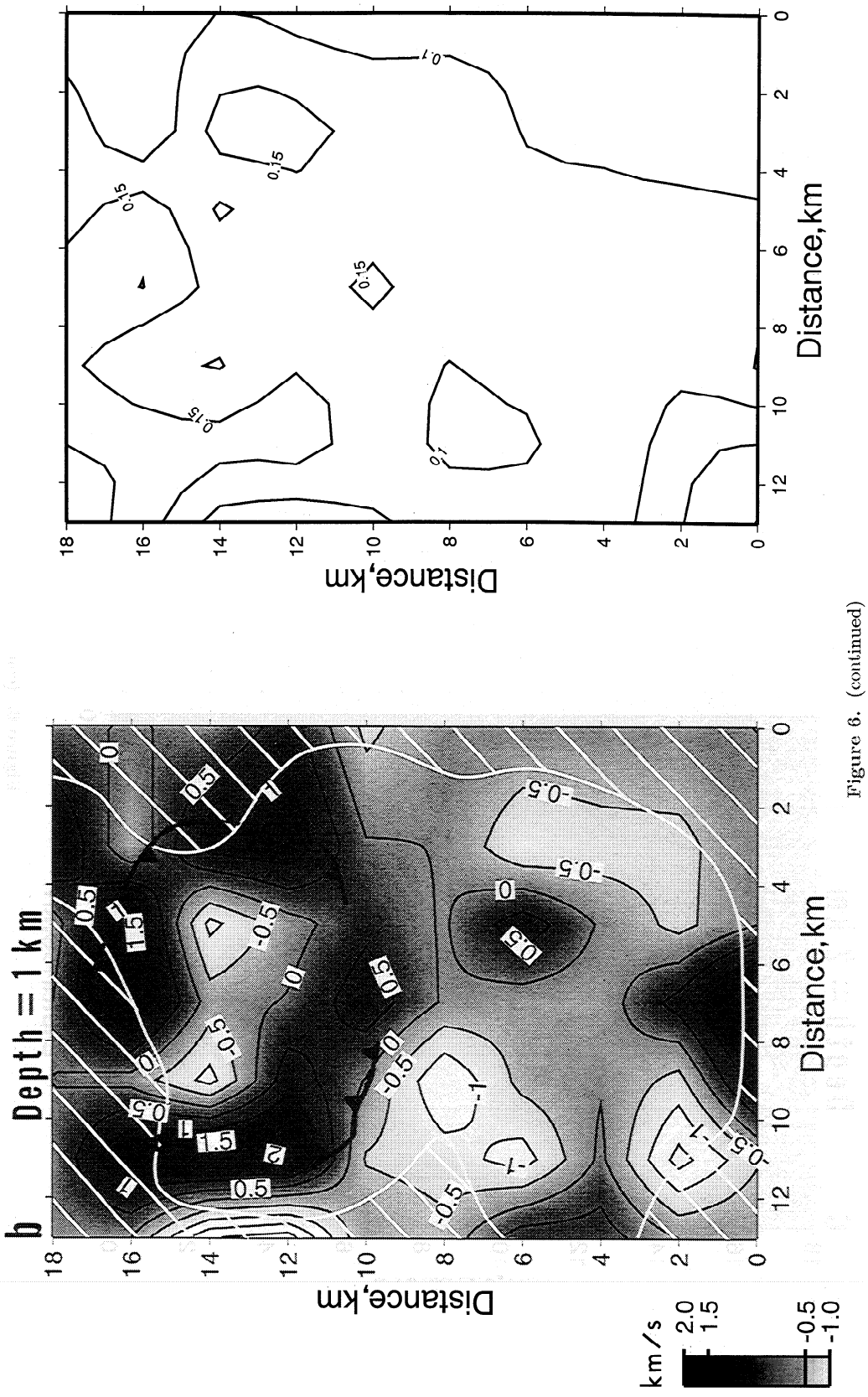

Figure 6. (continued)

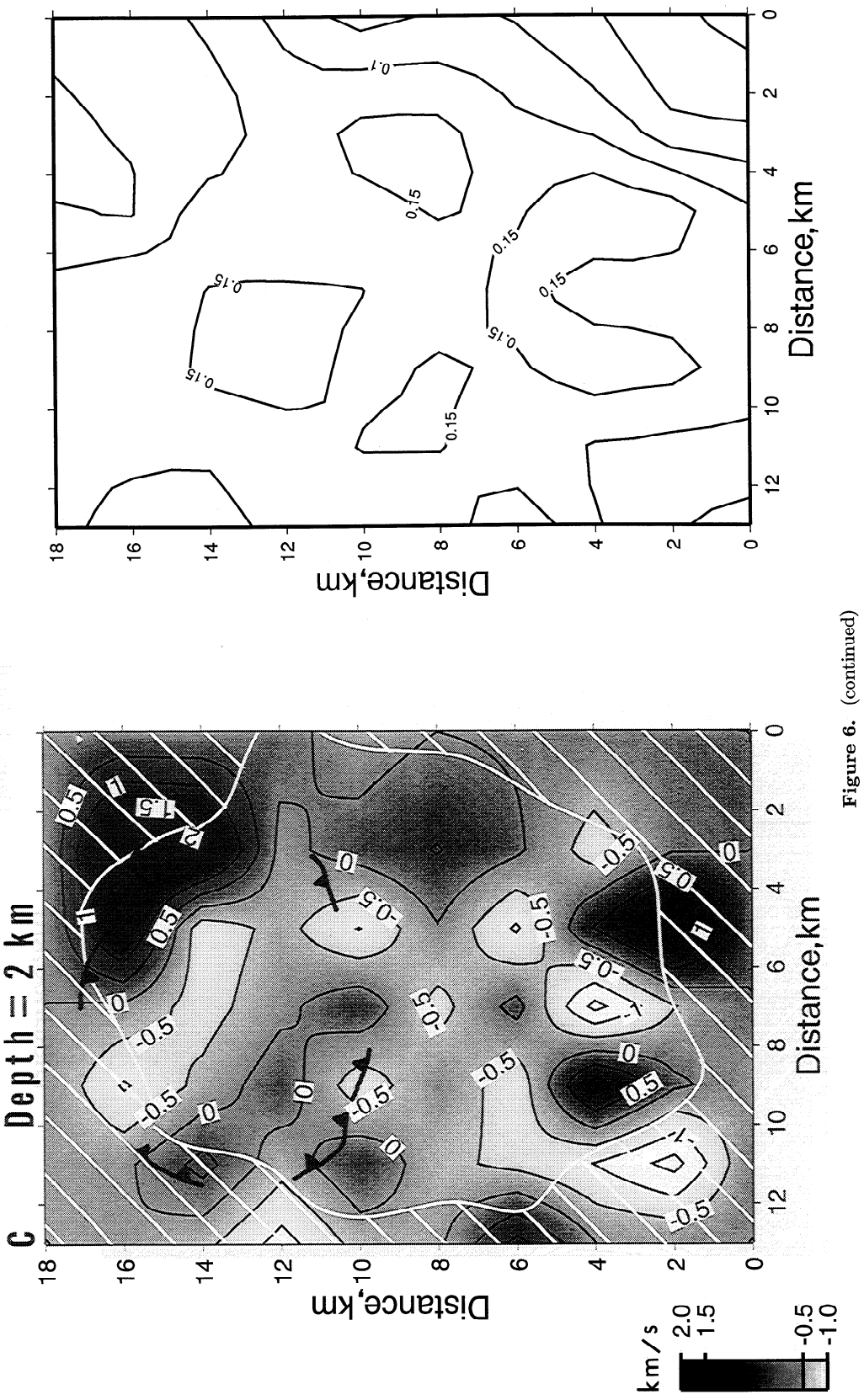

Figure 6. (continued)

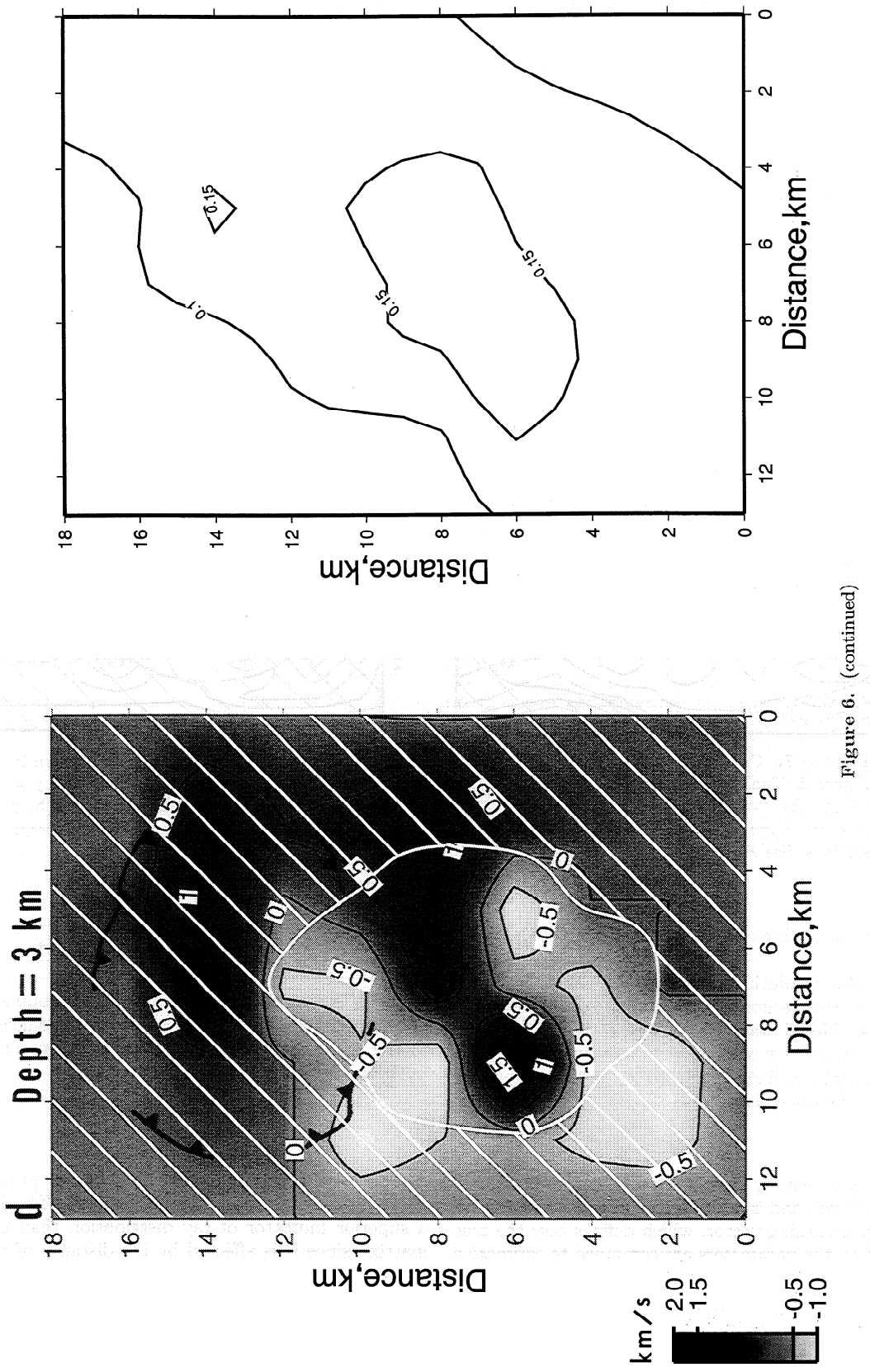

Figure 6. (continued)

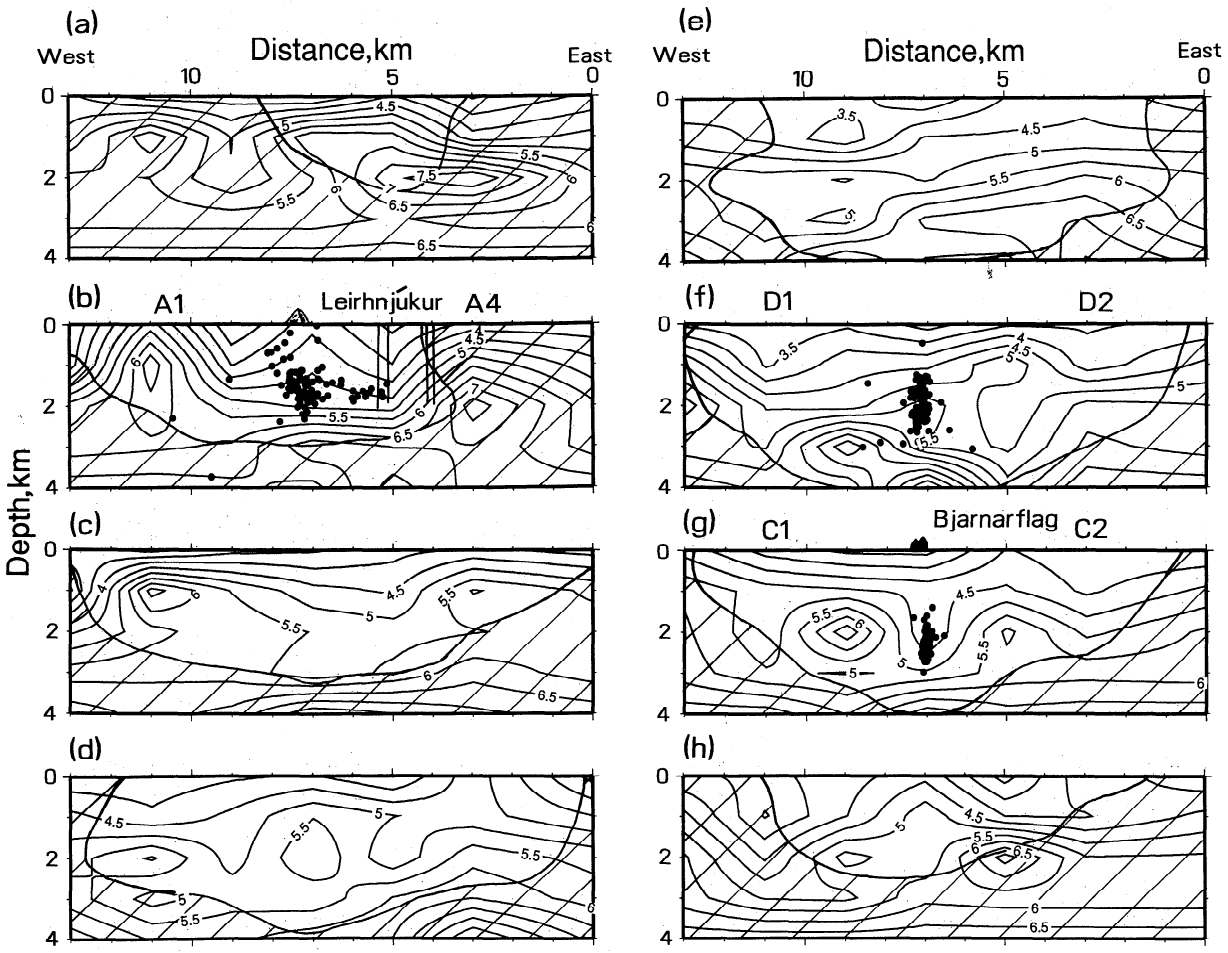

Figure 7. Cross sections from west to east through the velocity model. Lines of section are shown in Figure 2. The contour interval is 0.5 km s^{-1}. Poorly resolved areas (DWS < 50) are hatched. (a) y = 16 km, (b) y = 14 km, (c) y = 12 km, (d) y = 10 km, (e) y = 8 km, (f) y = 6 km, (g) y = 4 km, (h) y = 2 km. Hypocenters of events relocated using the three-dimensional crustal model are shown on some sections. See Figure 8d for lines of section.

twice this, or 0.3 km s^{-1}, throughout most of the study volume.

Parameter resolution expresses the degree to which each parameter estimate is contaminated by the values of others. Nodal wave speeds are estimated at each iteration by linearly combining the observations, which are assumed to be linearly related to the true parameter values by the operation

$$\hat{x} = R\overline{x}, \tag{1}$$

where $\hat{x}$ is the vector of estimated values, R is the resolution matrix, and $\overline{x}$ is the vector of true values. Each row is an averaging vector, which defines how the true values of all the parameters are combined to estimate a single parameter, and therefore they describe internodal contamination. The compactness of each averaging vector is a good indicator of the scale of features that can actually be resolved. We use the derivative weight sum (DWS) to assess compactness of the averaging vectors [*Toomey and Foulger*, 1989]. The DWS is defined as

$$\mathrm{DWS}(\alpha_n) = N \sum_{\text{rays}} \int_{\text{path}} \omega_n(\overline{x}) ds, \tag{2}$$

where N is a normalization factor that accounts for the volume influenced by α_n, is the influence coefficient used in the linear interpolation and depends on coordinate position. It is defined as

$$\omega_n(\overline{x}) = \frac{\partial V(\overline{x})}{\partial \alpha_n}. \tag{3}$$

A large DWS indicates that the velocity at the grid point is based on a large body of data. The DWS is a superior indicator of ray distribution than the "hit matrix" since it is affected by the distance of the rays from the velocity node. Empirical studies indicate that a DWS of 50 km or greater corresponds to a compact averaging vector with a spread of up to about 2 km [*Toomey and Foulger*, 1989]. Those parts of the final model resolved more poorly than this are hatched in Figures 6 and 7. These volumes are peripheral to the

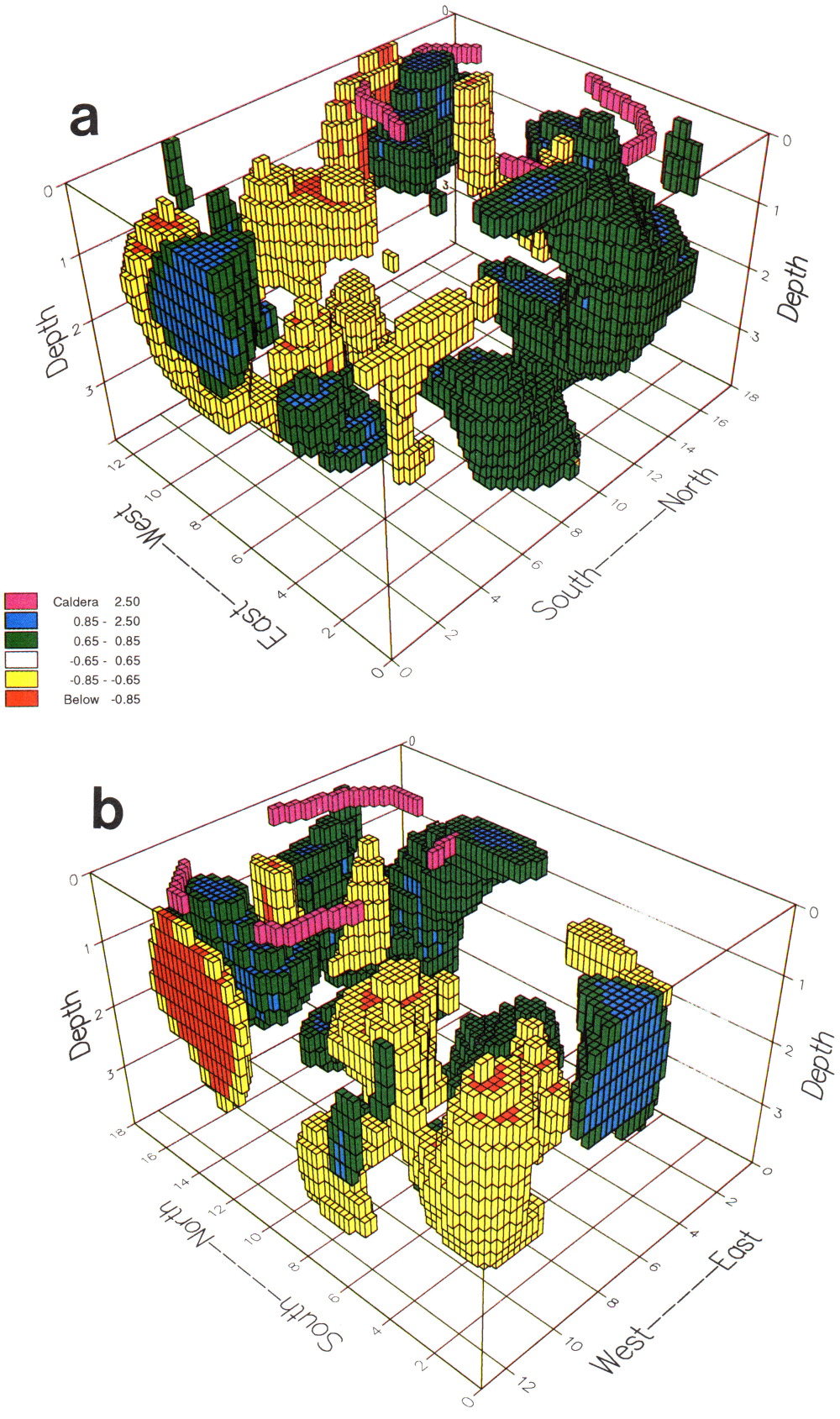

Plate 1. Three-dimensional perspective diagrams of velocity differences from the refined one-dimensional model. Velocity differences from the average for each depth are given in kilometers per second. (a) View from the southeast. (b) View from the southwest.

study volume, are constrained by few data, and are therefore also intuitively the least reliable parts of the model.

The uniqueness of the results is the stability of the final model as the input data and inversion parameters are varied. Inversions performed varying the starting crustal model, nodal spacings, and damping value within reasonable values all gave broadly similar results. This indicates that the broad features of our final model are stable and that it is unlikely that substantially differing, reasonable minima exist in our data set.

The most important question concerns the accuracy of the final results, i.e., how closely they approximate the truth. This is also the most difficult problem to address since the truth is never known exactly for field experiments. A number of studies have been performed using synthetic data generated using a known model, and these have confirmed the validity of the method for suitable experimental setups [e.g., *Kissling*, 1988; *Thurber*, 1981]. In the case of field experiments, the best approach is to compare the results with those from independent geological and geophysical work. Good correlation exists between some major features of our final model and information from drilling, gravity studies and surface geological mapping (see discussion section below). Smaller features of the model that are unsupported by independent evidence should be considered to be less reliable.

Results

Overall structure. Our refined one-dimensional velocity model differs systematically from the original model based on regional-scale refraction lines inasmuch as it contains higher velocities at all depths (Figure 4). It agrees well with models from other simultaneous inversion studies of spreading segments in Iceland [*Toomey and Foulger*, 1989; *Bjarnason et al.*, 1993], and with the results of a recent refraction profile within the Krafla caldera (B. Brandsdóttir, unpublished data, 1993), taking into consideration that our 0-depth velocities correspond to sea level, whereas the Krafla area is at an elevation of about 500 m above sea level.

High-velocity bodies. At 1 km depth (Figure 6b), three significant high-velocity volumes are imaged, underlying the western, northern, and eastern edges of the Krafla caldera. The western anomaly, centered at (11,14,1) has velocities up to about +2 km s^{-1} higher than the surrounding crust (i.e., velocities up to 6.5 km s^{-1}). It extends from the surface down to about 2 km depth (Figure 7b and Plate 1). The eastern anomaly extends from the surface at about (3,10,0) down to 2 km depth, where it reaches its maximum extent at about (3,16,2) and its maximum velocity anomaly of about +2 km s^{-1}. The northern anomaly extends from about (6,16,1), where it displays velocity anomalies of up to +1.5 km s^{-1}, to 2 km depth. There it merges with the eastern anomaly. The western and eastern bodies correlate qualitatively with residual Bouguer gravity highs of up to about 5 milliGals around the caldera rim (Figure 3). The northern body does not correlate well with the gravity field and is more poorly resolved, so it should therefore be considered less reliable. It is interesting to note that beneath the caldera rim, high-velocity bodies appear to define a ring structure at 1 km depth, which is fragmented at deeper and shallower depths.

A fourth high-velocity body is imaged in the south of the area and also has velocity anomalies of up to +2 km s^{-1}. It is centered at about (7,0,1), lies immediately beneath the ash cone Hverfjall (Figure 2) and extends from the surface down to about 2 km depth. Because it is on the periphery of the imaged volume, its lateral extent cannot be resolved to the south. It is well-resolved at 0 and 1 km depth, and the model covariances for this volume suggest that it is statistically significant. However, no supporting geophysical evidence is available so it should be regarded as less reliable than the western and eastern high-velocity bodies beneath the caldera rim.

Low-velocity bodies. Five volumes of relatively low velocity were imaged. The body with the most extreme velocity contrast underlies the Bjarnarflag well field within the Námafjall geothermal area. It reaches its minimum at 2 km beneath the well field at (7,4,2) and has velocity anomalies up to −1.5 km s^{-1} (Figure 7g). A significant low-velocity body lies within the Krafla caldera and extends from about 2 km depth, centered at (8,14,2), to the surface in the form of two pipes with velocity contrasts of up to −1 km s^{-1} (Figures 6a, 6b, and 7b and Plate 1). They crop out on the western flank of Mount Krafla (5,14,0) and about 1 km west-northwest of Leirhnjúkur (9,14,0). In between them, velocities are slightly higher. This structure is qualitatively mirrored by the residual Bouguer anomaly field, which indicates an isolated Bouguer high in the center of the caldera at Leirhnjúkur, flanked by lower gravity values (Figure 3). The structure inside the Krafla caldera could also be described as a low-velocity body with a small, high-velocity core underlying Leirhnjúkur in the depth range 0-2 km.

Bodies with smaller velocity anomalies occur in between the caldera and the Námafjall geothermal area to the south. Two are visible at 1 km depth. One is centered at about (10,8,1), is about 4 km in diameter, and has a velocity anomaly of up to −1 km s^{-1} (Figure 6b). The other extends from about (4,2,1) to about (2,6,1) and has a velocity anomaly up to −0.7 km s^{-1}. A third minor low-velocity body is imaged, centered at about (7,5,0). It has a velocity anomaly up to −0.7 km s^{-1}. The latter two bodies correlate with relatively low gravity values, which suggests that they may be reliable (Figure 3).

Temporal and Spatial Distribution of Local Earthquakes

Temporal Distribution

During the 95 days that the network was operated, 489 earthquakes locatable inside the network were re-

corded. The seismic rate for the whole area and the rates in different parts of the area were fairly continuous with time. No major swarms occurred during the monitoring period.

Location Method

The initial HYPOINVERSE [*Klein*, 1978] locations were improved in two stages. First, the whole earthquake set was relocated using the refined one-dimensional model based on early, simultaneous inversion results. Second, the events were relocated using the three-dimen- sional crustal model obtained from the simultaneous inversion. (This was done without performing additional iterations of the crustal structure.) The effects on the computed locations of successive refinements to the crustal model are illustrated in Figures 8 and 9.

Final Locations

The final locations calculated using the three-dimensional crustal structure show that local seismicity during the monitoring period was most intense beneath the Bjarnarflag well field in the Námafjall geothermal area (Figures 7g and 8d). Here it forms a tight epicentral cluster less than 500 m wide. Activity extended 4 km NNE along the fissure swarm from Bjarnarflag in a narrow linear zone, referred to here as the "dike zone" activity (Figures 8d and 7f). An aseismic "gap" about 3 km long separates the northernmost end of the dike zone activity from the diffuse cluster of earthquakes beneath the Krafla caldera. The most active central part of this cluster directly underlies the geothermally altered ridge Leirhnjúkur (Figures 7b and 8d).

The events occupy the depth range 0-3 km (Figure 9d). The dense cluster beneath the Bjarnarflag well field lies between 1.4 and 2.8 km depth (Figure 9d) and is widest at about 2.5 km depth, where it is about 400 m wide along the strike of the fissure swarm and 300 m wide perpendicular to it (Figures 7g and 9d). It is bounded sharply to the north by a subvertical plane that intersects the surface north of the well field. The sharpness of this contact suggests that the relative location error of the earthquakes may be as little as 100 m horizontally.

Along the dike zone the events occupy the depth range 1.2-3.1 km (Figures 7f and 9d). The apparent width of the seismic zone perpendicular to the fissure swarm is about 500 m (Figure 7f). Beyond the seismic gap, the cluster of events that underlie Leirhnjúkur occupies the depth range 0-2.3 km (Figures 7b and 9d). The densest part of this cluster lies at a depth of approximately 1.8 km and has a diameter of about 700 m.

Effect of Crustal Model Refinements on Event Locations

The effects on the locations of refining the crustal model were studied by comparing the locations obtained using the original one-dimensional model, the refined one-dimensional model and the three-dimensional model (Figures 8 and 9). Improving the one-dimensional model introduces a systematic change, and a largely systematic effect on the event locations would be expected. Moving to the three-dimensional model produces a less systematic change and would be expected to have a more complicated effect on the locations.

Improving the one-dimensional model generally resulted in epicentral movements of no more than about 500 m, which is of the same order as the horizontal error (the 32% probability range) in the original HYPOINVERSE locations [*Klein*, 1978] (Figure 8b). The epicenters of events in the Bjarnarflag cluster and the dike zone moved systematically northwards by about 100–200 m. Most of the events shallowed by 600–700 m, which in many cases is larger that the ERZ (the error in the vertical) of the HYPOINVERSE locations (Figure 9b).

Relocation using the three-dimensional model resulted in the events in the Bjarnarflag cluster moving westwards by an average of about 200 m (Figure 8c) and a further shallowing by about 500 m of the deepest events and somewhat less of the shallower events (Figure 9c). Events to the south of Bjarnarflag moved northwards by about 500 m. Within the dike zone the events generally migrated westward by 200–500 m. Within the caldera the events in the Leirhnjúkur cluster moved unsystematically. Many events moved in towards the center of the cluster and shallowed by 500 m to 1.0 km, though this effect was not as systematic as occurred by refining the one-dimensional model only.

The major effect on the epicentral locations of refining the original refraction-based crustal model to a three-dimensional model is the systematic NW movement by 200–300 m of the events in the Bjarnarflag cluster and the dike zone. These seismic volumes also became narrower normal to the fissure swarm, and they and the Leirhnjúkur cluster shortened parallel to the fissure swarm. The Bjarnarflag cluster became compacted vertically, occupying the depth range 1.9-2.8 km compared with the original 2-4 km, and the region of maximum width shallowed from about 2.7 to 2.2 km (compare Figures 9a and 9d). Activity within the dike zone was also compacted and the minimum depth of the events was decreased by about 500 m from 1.7 to 1.2 km.

The calculated spatial distribution of events beneath Leirhnjúkur changed considerably as a result of the crustal model refinements. The vertical extent reduced from 0-3.5 km to 0-2.3 km and an apparent northward dipping lineation, which is visible in Figure 9a, was subdued (Figure 9d).

The significance of the location changes resulting from use of the three-dimensional model may be assessed either statistically, using errors calculated from the data or logically using independent constraints. The largest change is the shallowing of many calculated hypocenters by about 1 km as a result of the systematic increase in velocity of the whole structure, and these revised depths are only as reliable as the revised crustal model. As discussed above, our final crustal model is robust, constrained by a large body of data, reduced

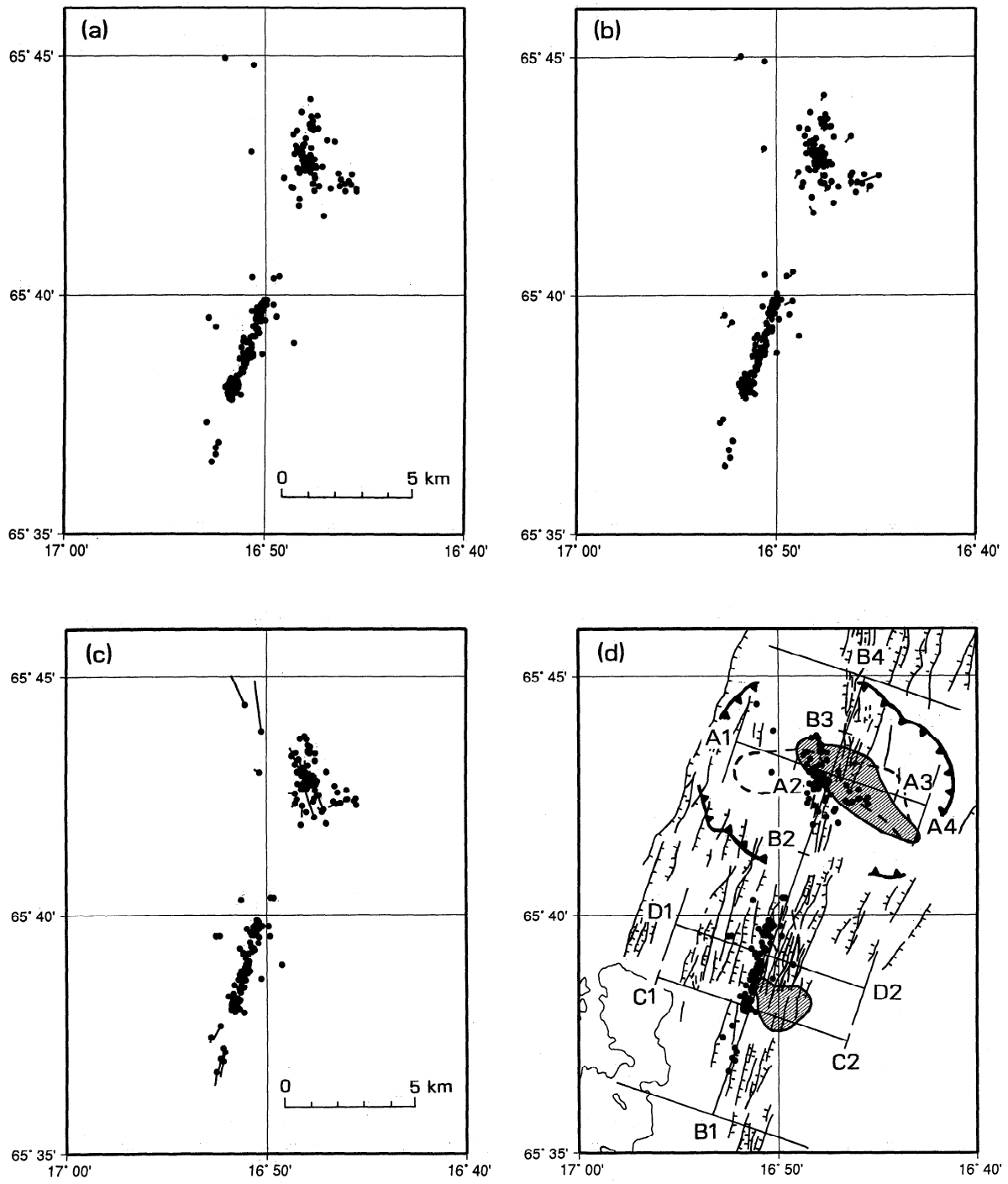

Figure 8. Epicenters of earthquakes used in the simultaneous inversion. (a) Locations obtained using HYPOINVERSE [*Klein*, 1978] and one-dimensional crustal model derived from regional refraction profiles (P. Einarsson, personal communication, 1985). All events have ERH and ERZ (errors in the horizontal and vertical) <1.0 km. (b) Migration of locations resulting from using the refined one-dimensional model. Vectors emanating from the epicenters indicate how the locations moved from the original position (tail) to the new position (dot). (c) Migration of locations resulting from replacing the refined one-dimensional model with the three-dimensional model. Vectors emanating from the epicenters indicate how the location moved. (d) Final locations obtained using the three-dimensional model. Faults and fissures of the Krafla fissure swarm are shown, along with the caldera rim. Shading denotes the geothermal areas and dashed lines indicate the surface projections of the magma lobes [from *Einarsson*, 1978]. Solid line indicates the shore of Lake Myvatn. The lines of sections shown in Figures 7, 9, and 13 are indicated.

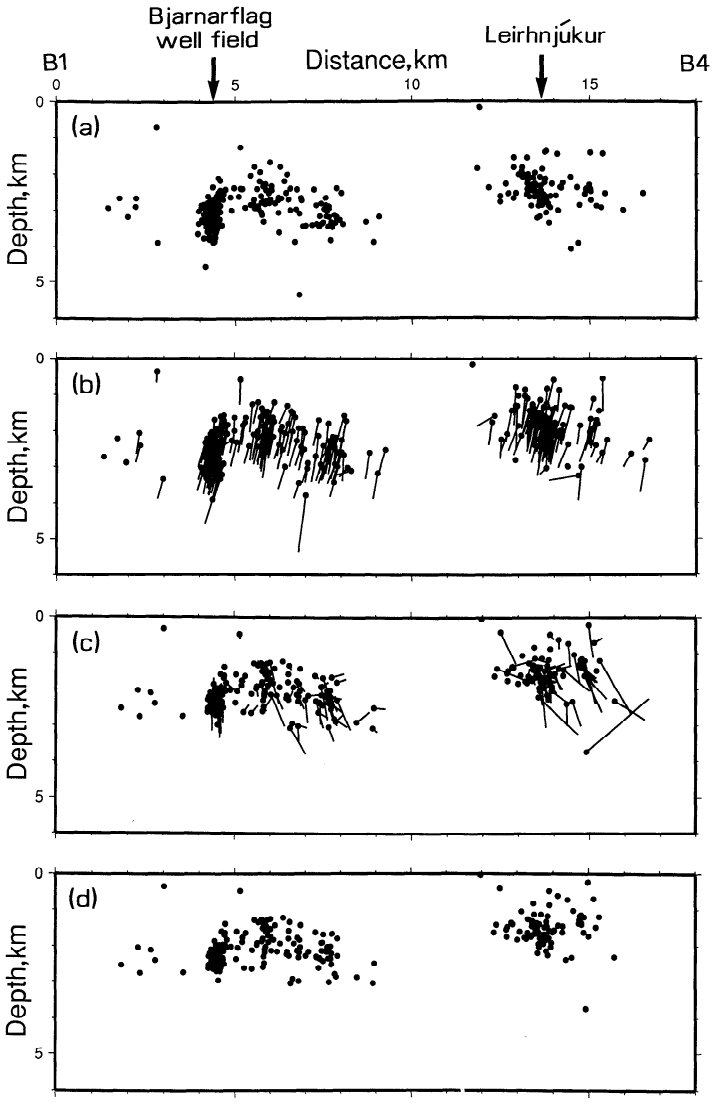

Figure 9. Hypocenters of earthquakes used in the simultaneous inversion, along the section B1-B4 (Figure 8d). No vertical exaggeration. (a) Locations obtained using HYPOINVERSE [*Klein*, 1978] and a one-dimensional crustal model derived from modeling nearby refraction lines (P. Einarsson, personal communication, 1985). (b) Migration of locations resulting from replacing the original one-dimensional model with the refined one-dimensional model. Vectors emanating from the hypocenters indicate how the locations moved. (c) Migration of locations resulting from replacing the refined one-dimensional model with the three-dimensional model. Vectors emanating from the epicenters indicate how the location moved. (d) Final locations obtained using the three-dimensional model.

the data variance to the estimated data error level, and is in good agreement with a local refraction study and the gravity field. The general, systematic shallowing of the events is therefore well supported.

The degree of clustering of events is a nonstatistical indication of the relative accuracy of locations. Repeated earthquakes often occur in small volumes, but small random errors in the calculated locations make those volumes appear larger than they actually are. Increased clustering may thus be viewed as evidence for improvement in the locations. The events located using the three-dimensional crustal model cluster much more closely in space than those located using the original one-dimensional model, particularly in depth (Figure 8d). The level of clustering gives some idea of the relative location accuracies of the events, which varies throughout the network.

The absolute accuracies can only be assessed by relocating events with known hypocenters and origin times. Two of the total of six explosions were detonated centrally within the network and close to the seismogenic volumes. Epicenters calculated for them using both the original one-dimensional model and the three-dimensional model were within a few hundred meters and

hypocentral depths were within 1 km of the true values. Although the locations changed little, the average RMS residual for the explosions reduced from 0.183 s before inversion to 0.060 s after inversion. Surface explosions are not an ideal indicator of absolute earthquake location accuracies, since they sample only the shallow layers. However, they provide the best indication available of absolute accuracy.

Magnitude History and b Values

A coda length magnitude scale is available for the permanent Icelandic seismograph station RI, operated by the University of Iceland (Figure 2). This had been derived by comparison with the body wave amplitude magnitude scale of the World-Wide Standard Seismograph Network (WWSSN) station at Akureyri and downward extrapolation to smaller magnitudes (P. Einarsson, personal communication, 1985). Coda length magnitude scales were derived in a similar way for three stations of our temporary network by comparison with station RI [*Arnott*, 1990].

Figure 10 illustrates how events of different magnitudes are distributed in time. There is very little evidence for swarm activity, and many of the events are technically mainshocks [*Sykes*, 1970]. The largest events occurred in the Bjarnarflag cluster, where five events of $M_{IL} > 1.0$ and two events of $M_{IL} > 2.0$ were located. Within the Krafla caldera, only three events occurred with $M_{IL} > 1.0$ and no events with $M_{IL} > 2.0$ occurred. In the dike zone, no events with $M_{IL} > 1.0$ occurred, and all but one event had magnitudes $M_{IL} < 0.2$.

We studied spatial and temporal variations in the b value [*Gutenberg and Richter*, 1941], which is half the fractal dimension of the seismic activity [*Turcotte*, 1993, p. 37]. Variations in b are thought to be related to inhomogeneity of the crust, or changes in the state of stress (b inversely proportional to stress) [*Scholz*, 1968]. Such variations would be expected in areas of inhomogeneous crustal structure or different earthquake generating processes.

Frequency-magnitude plots for the whole data set and for the Bjarnarflag, dike zone, and Krafla caldera subsets are shown in Figure 11. Figure 12 compares b values calculated for the linear part of the plots, i.e., that part above the detection threshold, using the maximum-likelihood method [*Page*, 1968].

A value of $b = 0.77 \pm 0.10$ was obtained for the whole area and is not significantly different at the 1σ level from the value of 0.84 ± 0.29 obtained by *Ward et al.* [1969] for the Krafla area using P wave amplitudes. If the seismic rate during the monitoring period was typical, the magnitudes of the expected daily and yearly events are approximately $M_{IL} = -0.4$ and 3.2, respectively.

The value of b for the dike zone (1.25 ± 0.30) is significantly different at the 1σ level from that of the Bjarnarflag area but not from the Krafla caldera. If b is inversely related to stress, it might be concluded that stress along the dike zone is lower than beneath the Bjarnarflag well field.

Discussion

Genesis Process

Our study was conducted immediately following a decade of tectonic activity and spreading in the Krafla volcanic system. It is therefore possible that the seismicity reported here resulted from continuing tectonic activity. This explanation is unlikely, however, since the earlier, tectonic seismicity comprised short, intensive swarms accompanying dike injections and magma chamber inflation [e.g., *Björnsson et al.*, 1979]. The b value of 0.77 ± 0.10 we obtain for our data set also contrasts greatly with that of 1.7 ± 0.2 obtained by *Einarsson and Brandsdóttir* [1980] for a swarm accompanying a dike injection north of the volcano in 1978. At the time of our study, the system was tectonically quiescent

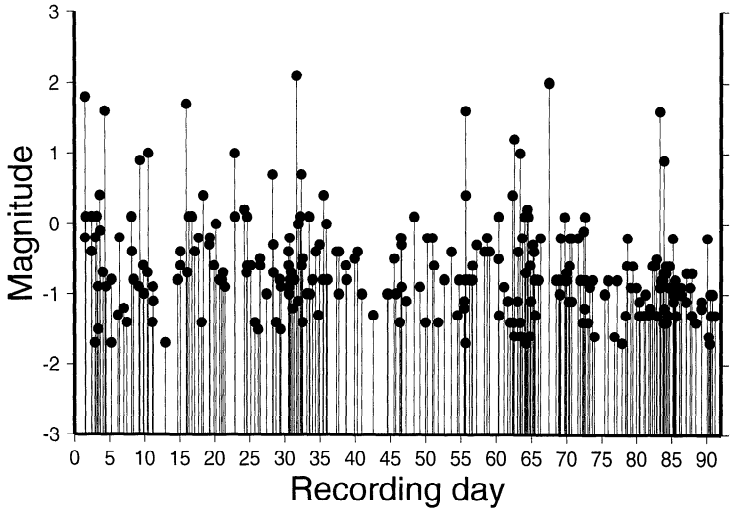

Figure 10. Temporal distribution of local earthquakes plotted against M_{IL} (local Icelandic) magnitude for the entire data set.

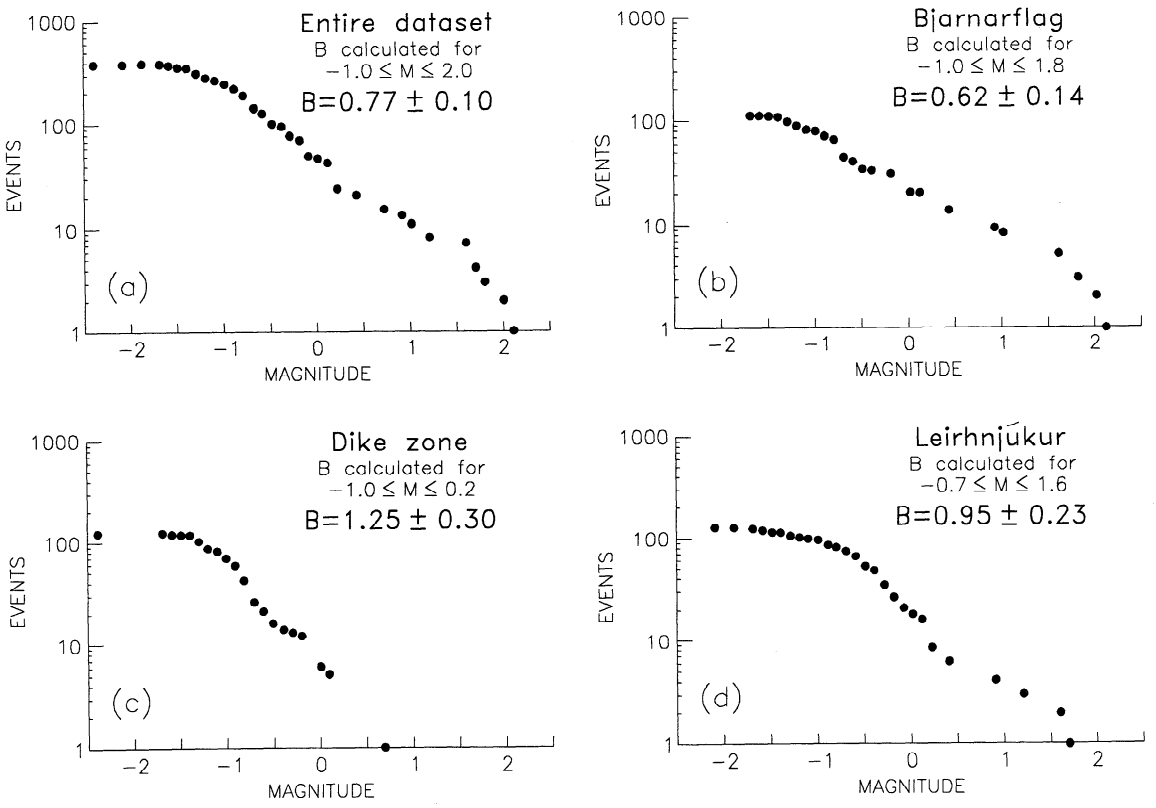

Figure 11. Cumulative frequency: magnitude plots for (a) the entire data set, (b) the Bjarnarflag cluster, (c) the dike zone events, and (d) the events beneath Leirhnjúkur.

(e.g., tilt rates were low), and the events we recorded were continuous and small magnitude. We therefore reject the hypothesis that the activity resulted from a continuation of the spreading episode.

Continuous, small-magnitude earthquake activity characterizes the high-temperature geothermal areas of Iceland, and it has been proposed that it is induced by geothermal processes [*Ward et al.*, 1969; Einarsson and Sæmundsson, 1987; *Foulger*, 1988a; *Foulger and Long*, 1984]. This is the explanation we favor for the seismicity we report here. This conclusion is supported by the observation that some events have nonshear focal mechanisms [*Foulger et al.*, 1989; *Arnott*, 1990; *Arnott and Foulger*, this issue], a phenomenon observed in other Icelandic geothermal areas and attributed to geothermal heat loss [*Foulger*, 1988b].

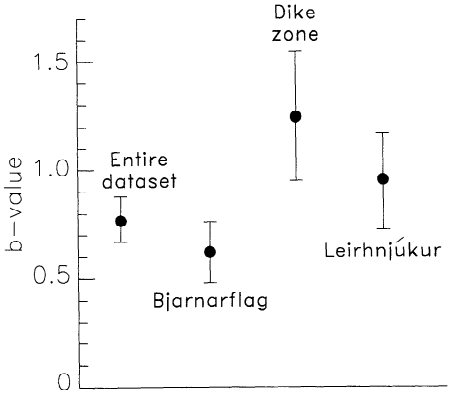

Figure 12. The variation in b value over the area. Vertical bars indicate the 1σ standard error for each value.

Effect of Crustal Model Refinements on Calculated Earthquake Locations

Substituting a three-dimensional crustal model for the original one-dimensional refraction-based model resulted in relatively minor changes in calculated epicenters but major changes in focal depths. The calculated maximum depth of the earthquakes decreased by about 1 km from 3-4 km to 2-3 km. This illustrates that substantial mislocations may occur if a regional crustal structure is used to locate earthquakes in a local, anomalous area. Earlier estimates of hypocentral depths in the Krafla segment, especially those that used local stations and upgoing rays, may thus have been overestimated, e.g., earthquakes accompanying the September 1977 dike injection may have been substantially shallower than the 3-7 km reported [e.g., *Brandsdóttir and Einarsson*, 1979]. Hypocentral depth estimates for events in other anomalous, local areas made using regional crustal models may also contain errors from this source, e.g., studies of marine black smokers that use refraction-based crustal models.

Krafla Area

The earthquakes occurred mostly in the intrusive formation that underlies the surface subaerial lava and hyaloclastite layers and between the two low-velocity pipes imaged (Figures 7b and 13). They directly underlie Leirhnjúkur, in the center of the fissure swarm and between the two magma chamber lobes [*Einarsson*, 1978] (Figure 2), i.e., directly above the magma chamber roof pendant. This location also marks the center of magma chamber inflation [e.g., *Björnsson et al.*, 1979]. If the events are induced by geothermal cooling, then they define the hot rock body that fuels the Leirhnjúkur fumaroles. The seismic volume corresponds mainly to the lower, boiling zone of the geothermal reservoir. Temperatures measured in boreholes 1.5-2 km east of the main area of seismicity indicate temperatures of >250°C for this zone [*Ármannsson et al.*, 1987], though care should be exercised in extrapolating this directly to the volume beneath Leirhnjúkur since lateral temperature gradients may be very large in volcanic geothermal areas.

Several factors suggest that the volume directly beneath Leirhnjúkur is intensely fractured and may contain a magma conduit that provides a pathway for the flow of magma when the chamber discharges. (1) Continuous earthquake activity occurs there and may maintain a system of permeable cracks. (2) A WNW trending fault passing through the center of the seismic volume has been identified by drilling [*Ármannsson et al.*, 1987]. (3) The roof pendant in the magma chamber may have resulted from localized, deep cooling by geothermal fluids circulating through fractures. (4) This locality overlies the recent center of inflation of the magma chamber and thus experiences great extensional stress during magma-chamber inflation. (5) It is in the center of the fissure swarm where extensional stresses and fracturing are probably greatest and intensive dike in-

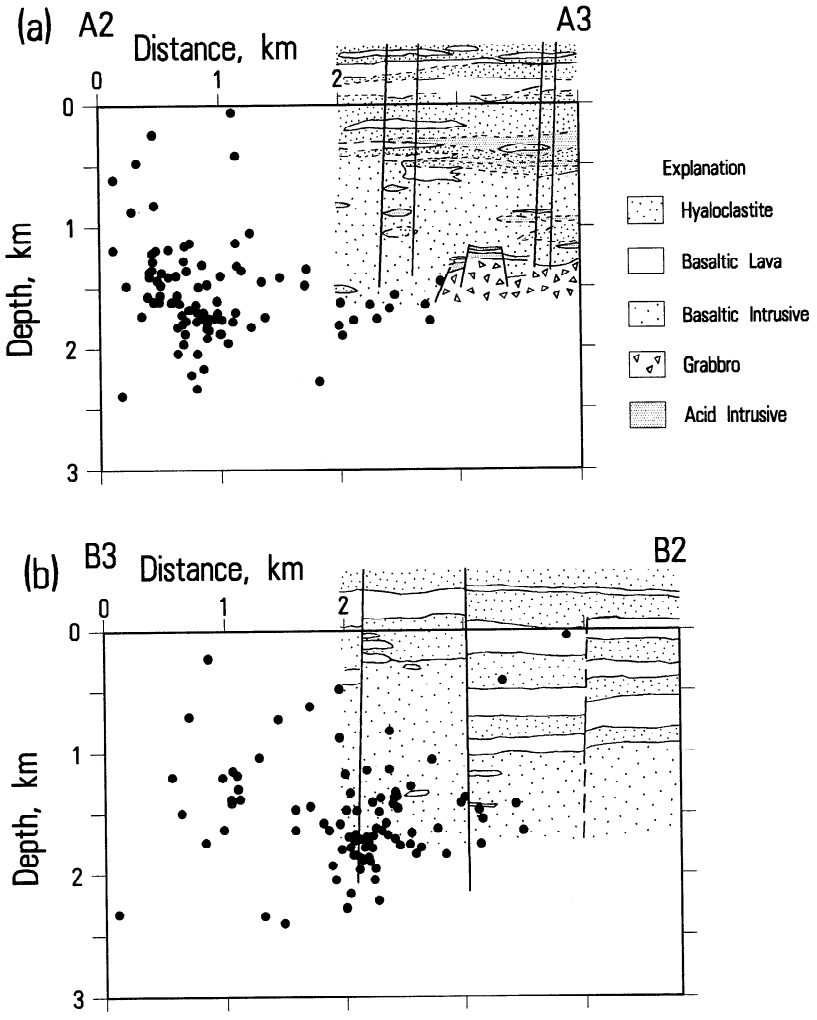

Figure 13. Plot of earthquake hypocenters and geology as deduced from borehole studies (adapted from *Ármannsson et al.* [1987]). (a) WNW-ESE section A2–A3, vertical exaggeration 1.2: 1. Vertical lines indicate drill holes. (b) NNE-SSW section B3–B2, vertical exaggeration 0.6: 1. Vertical lines indicate faults. See Figure 8d for locations of lines of section.

trusion occurred recently. (6) Leirhnjúkur was the site of fissure eruptions both during the recent episode and that of a historic episode 1724-1729.

The simultaneous inversion detects relatively low velocities beneath the caldera, in particular, two vertical columns on either side of Leirhnjúkur from 0 to 2 km depth where they merge together in the same volume as the seismicity. The eastern column coincides with the most intensively exploited part of the geothermal reservoir, on the western slopes of Mount Krafla, and is interpreted as a hydrothermally altered volume. It represents the main pathway of geothermal fluid flow to the boreholes. Seismicity at the base of this zone suggests cooling there in addition to that beneath Leirhnjúkur. The low-velocity column west of Leirhnjúkur may also represent hydrothermal alteration, but the absence of long-lived surface heat loss or low resistivity there suggests that this zone is currently geothermally inactive.

Large, high-velocity bodies imaged beneath the western and eastern parts of the caldera ring fault correlate with Bouguer gravity highs and indicate high-density bodies. Boreholes have encountered gabbro at depths greater than 1800 m beneath the eastern part of the caldera. A granular gabbro at a depth of about 2 km and pressure of about 5×10^6 Pa would have a seismic velocity of about 7.1 km s^{-1} [*Kroenke et al.*, 1976]. This is higher than the 6.5–7.0 km s^{-1} imaged, but slightly depressed velocity estimates may result from velocity averaging in the inversion, uncertainties, and the in situ rock differing from the homogeneous gabbro studied by *Kroenke et al.* [1976]. Given these uncertainties, the velocities we image are consistent with gabbro at that depth. The high-velocity bodies may represent intrusions that occurred in the neighborhood of the caldera ring fault because it provided a weak zone. Gabbro intrusions are exposed in the eroded roots of old, extinct central volcanoes in Iceland which is consistent with our interpretation [e.g., *Walker*, 1974].

The high-velocity body that underlies Hverfjall in the south of the area could also be a gabbroic intrusion. Hverfjall is an ash cone with a resurgent dome, and the intrusion may have accompanied its formation. However, this feature is peripheral to the model, therefore poorly resolved, and should be considered tentative.

Námafjall Area

Within the Námafjall geothermal area, the majority of the earthquakes lay in a tight cluster at 1.4–2.8 km depth beneath the Bjarnarflag well field. This cluster has an east-west width of about 300 m and has a sharp northern edge. The b value for these events is relatively low (0.62 ± 0.14), suggesting a high-stress state. The seismicity coincides with a low-velocity zone imaged by the simultaneous inversion (Figure 7g).

The coincidence of the seismicity and the well site suggests that some earthquakes may be induced by geothermal fluid mining activities, as they are, for example, at The Geysers, California [*Stark*, 1992], though detailed correlations of seismicity and development are unavailable. This is supported by the character of the stress field, derived from focal mechanisms, which showed no preferred orientation of the axes of principal stress, suggesting that systematic tectonic forces are not responsible for the earthquakes [*Arnott and Foulger*, this volume]. In addition, the few days of preproduction monitoring available suggest a higher seismic rate in the Krafla caldera than the Námafjall area [*Ward et al.*, 1969; *Ward and Björnsson*, 1971], whereas that situation was reversed in 1985. This feature of the seismicity in this volcanic system contrasts with that of other geothermal areas in Iceland, e.g., the Hengill area, where all the seismicity appears to be induced by natural heat loss [*Foulger*, 1988b]. Geothermally induced seismicity is known elsewhere, however, e.g., in The Geysers geothermal area, California [*Eberhart-Phillips and Oppenheimer*, 1984].

In addition to heat, large volumes of fluid are being withdrawn from beneath Bjarnarflag. Possible induction processes therefore include both thermal contraction and volume removal. In either case, the seismic volume is the source of the heat being mined at Bjarnarflag. The low velocities imaged are probably due to hydrothermal alteration. The sharp northern edge of the seismic volume projects up to the surface at the well field and may represent a fault along which geothermal fluids flow to the surface. Dikes injected in 1977 and 1980 passed through Bjarnarflag and continued 4 km to the south, and continued stress relaxation in the neighborhood of those dikes may thus also contribute to the 1985 seismicity there.

Dike Zone

The narrow, bladelike seismic zone at 1.2-3.1 km depth along the fissure swarm coincides with dikes injected southward in 1977 and 1980. This spatial correlation and the continuous nature of the earthquakes suggest that they result from an ongoing, natural process associated with the young dikes there. There is no evidence for geothermal activity at the surface, the total width of dikes injected was about 3 m [*Björnsson et al.*, 1979; *Björnsson*, 1985], and about 5 years elapsed between injection and our seismic monitoring. It is probable that the dikes and neighboring rock were thoroughly cooled by the time of our monitoring and that the earthquakes do not result from continued cooling. We suggest that they are associated with minor stress release on a small scale as the crust returns to equilibrium in the neighborhood of the new dikes.

Conclusions

1. After the cessation of major tectonism in the Krafla volcanic system in 1984, seismicity comprised continuous, small-magnitude earthquakes concentrated in the Krafla and Námafjall geothermal areas and the southerly zone of recent dike injection.

2. Crustal models based on regional refraction profiles may inadequately model local, anomalous areas and introduce serious errors into the computed focal depths of earthquakes. The use of a three-dimensional

crustal structure may significantly improve the resolution of structures such as seismically active faults.

3. High-velocity, high-density, gabbroic intrusions underlie the caldera ring fault.

4. Volumes with low seismic velocities beneath the geothermal areas are interpreted as zones of hydrothermal alteration and pervasive fracturing.

5. Seismicity beneath the Krafla system is confined to the 0-3 km depth interval and lies mostly within the boiling zone of the hydrothermal system.

6. The seismic rate during a 3-month monitoring period was one magnitude 3.2 event per year with a b value of 0.77 ± 0.10.

7. The seismic activity results dominantly from geothermal processes. The activity beneath the Bjarnarflag well field may also be partly induced by exploitation and by stress relaxation at the southern tip of recently injected dikes.

8. The seismic volume beneath Leirhnjúkur is probably highly fractured and may provide a pathway for magma flow out of the Krafla magma chamber during active periods.

9. Seismicity at the locus of recent dike injections indicates that the crust there had not completely returned to stress equilibrium after 5 years.

Acknowledgments. This project was financed by the Natural Environment Research Council (which also provided the field equipment), the National Energy Authority, Iceland, and a grant from the Icelandic Science Fund to the Science Institute, University of Iceland. It greatly benefited from cooperative work with Páll Einarsson, Axel Björnsson, and Lárus H. Bjarnason. Fred Klein, Bruce Julian, Ólafur Gudmundsson, and Bryndis Brandsdóttir refined the manuscript greatly.

References

Ármannsson, H., A. Gudmundsson, and B.S. Steingrimsson, Exploration and development of the Krafla geothermal area, *Jökull, 37*, 13–29, 1987.

Arnott, S.K., A seismic study of the Krafla volcanic system, Iceland, Ph.D. thesis, vii + 283 pp., Univ. of Durham, Durham, England, 1990.

Arnott, S.K. and G.R. Foulger, The Krafla spreading segment, Iceland, 2, The accretionary stress cycle and nonshear earthquake focal mechanisms, *J. Geophys. Res.*, this issue.

Bjarnason, I. T., W. Menke, O. G. Flovenz, and C. Caress, Tomographic image of the Mid-Atlantic plate boundary in southwestern Iceland, *J. Geophys. Res., 98*, 6607–6622, 1993.

Björnsson, A., Dynamics of crustal rifting in NE Iceland, *J. Geophys. Res., 90*, 10,151–10,162, 1985.

Björnsson, A., K. Sæmundsson, P. Einarsson, E. Tryggvason, and K. Grönvold, Current rifting episode in North Iceland, *Nature, 266*, 318–323, 1977.

Björnsson, A., G. Johnsen, S. Sigurdsson, G. Thorbergsson, and E. Tryggvason, Rifting of the plate boundary in northern Iceland 1975–1978, *J. Geophys. Res., 84*, 3029–3038, 1979.

Brandsdóttir, B., and P. Einarsson, Seismic activity associated with the September 1977 deflation of the Krafla central volcano in north-eastern Iceland, *J. Volcanol. Geotherm. Res., 6*, 197–212, 1979.

Eberhart-Phillips, D., Three-dimensional structure in northern California Coast Ranges from inversion of local earthquake arrival times, *Seismol. Soc. Am. Bull., 76*, 1025–1052, 1986.

Eberhart-Phillips, D., and D.H. Oppenheimer, Induced seismicity in The Geysers geothermal area, California, *J. Geophys. Res., 89*, 1191–1207, 1984.

Einarsson, P., S-wave shadows in the Krafla caldera in NE-Iceland, evidence for a magma chamber in the crust, *Bull. Volcanol., 41*, 1–9, 1978.

Einarsson, P., and B. Brandsdóttir, Seismological evidence for lateral magma intrusion during the July 1978 deflation of the Krafla volcano in NE-Iceland, *J. Geophys., 47*, 160–165, 1980.

Einarsson, P., and K. Sæmundsson, Earthquake epicenters 1982–1985 and volcanic systems in Iceland (map), in *"I hlutarins edli," Festschrift for Thorbjörn Sigurgeirsson*, edited by T. Sigfusson, Menningarsjodur, Reykjavik, 1987.

Francis, T.J.G., The detailed seismicity of mid-ocean ridges, *Earth Planet. Sci. Lett., 4*, 39–46, 1968.

Foulger, G.R., Geothermal exploration and reservoir monitoring using earthquakes and the passive seismic method, *Geothermics, 11*, 259–268, 1982.

Foulger, G.R., The Hengill triple junction, SW Iceland, 1, Tectonic structure and the spatial and temporal distribution of local earthquakes, *J. Geophys. Res., 93*, 13,493–13,506, 1988a.

Foulger, G.R., The Hengill triple junction, SW Iceland, 2, Anomalous focal mechanisms and implications for processes within the geothermal reservoir and at accretionary plate boundaries, *J. Geophys. Res., 93*, 13,507–13,523, 1988b.

Foulger, G.R., and R.E. Long, Anomalous focal mechanisms: Tensile crack formation on an accreting plate boundary, *Nature, 310*, 43–45, 1984.

Foulger, G.R., and D.R. Toomey, Structure and evolution of the Hengill-Grensdalur volcanic complex, Iceland: Geology, geophysics and seismic tomography, *J. Geophys. Res., 94*, 17,511–17,522, 1989.

Foulger, G.R., R.E. Long, P. Einarsson, and A. Björnsson, Implosive earthquakes at the active accretionary plate boundary in northern Iceland, *Nature, 337*, 640-642, 1989.

Gudmundsson, A., et al., The 1991 eruption of Hekla, Iceland, *Bull. Volcanol., 54*, 238–246, 1992.

Gutenberg, B., and C.F. Richter, Seismicity of the Earth, *Spec. Pap. Geol. Soc. Am. 34*, 1–133, 1941.

Karlsdóttir, R., G. Johnsen, A. Björnsson, O. Sigurdsson, and E. Hauksson, The geothermal area of Krafla: General report on geophysical research 1976-78 (in Icelandic), *Rep. OS/JHD-7847*, Natl. Energy Auth., Reykjavik, 1978.

Kissling, E., Geotomography with local earthquake data, *Rev. Geophys., 26*, 659–698, 1988.

Klein, F.W., Hypocenter location program HYPOINVERSE, *U.S. Geol. Surv. Open File Rep., 78-694*, 1978.

Klein, F.W., P. Einarsson, and M. Wyss, The Reykjanes Peninsula, Iceland, earthquake swarm of September 1972 and its tectonic significance, *J. Geophys. Res., 82*, 865–888, 1977.

Kroenke, L.W., M.H. Manghnani, C.S. Rai, P. Fryer, and R. Ramananantoandro, Elastic properties of selected ophiolitic rocks from Papua New Guinea: Nature and composition of oceanic lower crust and upper mantle, in *The Geophysics of the Pacific Ocean Basin and Its Margin, Geophys. Monogr. Ser.*, vol. 19, pp. 407–421, AGU, Washington, D.C., 1976.

Page, R., Aftershocks and microaftershocks of the great Alaska earthquake of 1964, *Bull. Seismol. Soc. Am., 58*, 1131–1168, 1968.

Ragnars, K., K. Sæmundsson, S. Benediktsson, and S.S. Einarsson, Development of the Námafjall area, northern Iceland, *Geothermics, Special Issue 2, 2*(1), 925–935, 1970.

Sæmundsson, K., An outline of the geology of Iceland, *Jökull, 29*, 7–28, 1979.

Sæmundsson, K., Calderas in the neovolcanic zones of Iceland, in *Eldur er í Nordri: Festschrift für Sigurdur Thorarinsson*, pp. 221–239, Sögufelag, Reykjavik, , 1982.

Scholz, C., The frequency-magnitude relation of microfracturing in rock and its relation to earthquakes, *Bull. Seismol. Soc. Am., 58*, 399–415, 1968.

Stark, M. A., Microearthquakes–A tool to track injected water in The Geysers reservoir, *Geotherm. Resourc. Counc. Spec. Rep. 17*, 111–120, 1992.

Stefánsson, V., The Krafla geothermal field, northeast Iceland, in *Geothermal Systems: Principles and Case Histories*, edited by L. Rybach and L.J.P. Muffler, pp. 273–294, John Wiley, New York, 1981.

Sykes, L.R., Mechanism of earthquakes and nature of faulting on the mid-ocean ridges, *J. Geophys. Res., 72*, 2131–2153, 1967.

Sykes, L.R., Earthquake swarms and seafloor spreading, *J. Geophys. Res., 75*, 6598–6611, 1970.

Thorarinsson, S., *On the Geology and Geophysics of Iceland: Guide to Excursions 60*, International Geological Congress, Reykjavik, 1960.

Thurber, C. H., Earth structure and earthquake locations in the Coyote Lake area, central California, Ph.D. thesis, Mass. Inst. of Technol., Cambridge, 1981.

Thurber, C. H., Earthquake locations and three-dimensional crustal structure in the Coyote Lake area, central California, *J. Geophys. Res., 88*, 8226–8236, 1983.

Thurber, C. H., Seismic detection of the summit magma complex of Kilauea volcano, Hawaii, *Science, 223*, 165–167, 1984.

Thurber, C. H., Analysis methods for kinematic data from local earthquakes, *Rev. Geophys., 24*, 793–805, 1986.

Thurber, C. H., Local earthquake tomography: velocities and V_p/V_s-Theory, in *Seismic Tomography: Theory and Practice*, edited by H.M. Iyer and K. Hirahara, pp. 563–583, Chapman and Hall, New York, 1993.

Toomey, D.R., and G.R. Foulger, Tomographic inversion of local earthquake data from the Hengill-Grensdalur central volcano complex, Iceland, *J. Geophys. Res., 94*, 17,497–17,510, 1989.

Toomey, D.R., S.C. Solomon, and G.M. Purdy, Microearthquakes beneath the median valley of the Mid-Atlantic Ridge near 23°N: Tomography and tectonics, *J. Geophys. Res., 93*, 9093–9112, 1988.

Turcotte, D.L., *Fractals and Chaos in Geology and Geophysics*, 221 pp., Cambridge University Press, New York, 1993.

Walker, G.P.L., The structure of eastern Iceland, in *Geodynamics of Iceland and the North Atlantic Area*, ed. L. Kristjánsson, Dordrecht, Holland, D. Reidel Publ. Do., 177–188, 1974.

Ward, P.L. and S. Björnsson, Microearthquakes, swarms and the geothermal areas of Iceland, *J. Geophys. Res., 76*, 3953–3982, 1971.

Ward, P.L, G. Palmason, and C. Drake, Microearthquake survey and the mid-Atlantic ridge in Iceland, *J. Geophys. Res., 74*, 665–684, 1969.

S. K. Arnott, Shell International Petroleum Company, Postbus 1, 7760 AA Schoonebeek Beekweg 33, The Hague, Netherlands.

G. R. Foulger, Dept. Geological Sciences, University of Durham, Science Laboratories, South Road, Durham, DH1 3LE, U.K. (email: g.r.foulger@durham.ac.uk)

(Received August 30, 1993; revised May 23, 1994; accepted June 8, 1994.)